Lithos 112 (2009) 367–381

Contents lists available at ScienceDirect

Lithos

journal homepage: www.elsevier.com/locate/lithos

Neoproterozoic adakitic rocks from Mopanshan in the western Yangtze Craton: Partial melts of a thickened lower crust

Xiao-Long Huang *, Yi-Gang Xu *, Jiang-Bo Lan, Qi-Jun Yang, Zheng-Yu Luo

Key Laboratory of Isotope Geochronology and Geochemistry, Guangzhou Institute of Geochemistry, Chinese Academy of Sciences, Guangzhou 510640, China

ARTICLE INFO

Article history:
Received 11 September 2008
Accepted 17 March 2009
Available online 28 March 2009

Keywords:
Hf isotope
Neoproterozoic
Adakitic rocks
Lower crust
Western Yangtze Craton
South China

ABSTRACT

The tectonic setting of South China during the Neoproterozoic remains a subject of debate. Neoproterozoic adakites from Xuelongbao and Datian along the western margin of the Yangtze Craton have been used to argue for an arc setting assuming that these rocks are the melting products of a subducted oceanic slab (Zhou, M.F., Yan, D.P., Wang, C.L., Qi, L., Kennedy, A., 2006a. Subduction-related origin of the 750 Ma Xuelongbao adakitic complex (Sichuan Province, China): Implications for the tectonic setting of the giant Neoproterozoic magmatic event in South China. Earth and Planetary Science Letters 248, 286–300.; Zhao, J.H., Zhou, M.F., 2007. Neoproterozoic Adakitic Plutons and Arc Magmatism along the Western Margin of the Yangtze Block, South China. The Journal of Geology 115, 675–689.). However, the slab-related petrogenetic model is unsuitable for the Neoproterozoic (782 ± 6 Ma) adakites from Mopanshan. The Mopanshan adakites are characterized by low MgO, Cr and Ni contents, high Rb/Sr and Sr/Y ratios and negative $\varepsilon_{Nd}(t)$ values (−2.06 to −0.43). These features, plus the presence of relict zircons (1.16–0.83 Ga) and Mesoproterozoic zircon Hf model ages (1.06–1.27 Ga), are inconsistent with a slab-melting origin, but favour an origin by melting of a thickened continental lower crust. It is likely that the crust associated with magma generation may have experienced continuous growth and reworking since the Sibao Orogeny. Sharing the main geochemical features with the Mopanshan rocks, the Xuelongbao and Datian adakites may also have been derived from a thickened lower crust. This interpretation casts doubts on the Neoproterozoic arc setting proposed for south China. Instead, the Neoproterozoic in south China may represent an intra-continental extensional setting.

1. Introduction

Adakites, characterized by high Sr/Y and low HREE, have been interpreted as typical melting products of subducted oceanic slabs (Defant and Drummond, 1990). If this interpretation is correct, adakites can be used as an indicator for tectonic setting. Unfortunately, it has been demonstrated that adakitic rocks can also be generated by partial melting of thickened lower crusts (e.g., Petford and Atherton, 1996; Chung et al., 2003; Wang et al., 2005) or delaminated lower crust (Xu et al., 2002; Wang et al., 2006a). Moreover, adakites can also be formed via fractionation of mafic magmas (Castillo, 2006). The potentially multiple origin of adakitic rocks suggests (e.g., Castillo, 2006; Wang et al., 2006a; Li et al., 2007a) that adakitic rocks cannot be used as an effective tectonic indicator unless there are independent lines of evidence.

In recent years, the Neoproterozoic tectonic setting in south China has been a subject of debate (e.g., Li et al., 2004a; Wang et al., 2004a,b; Li et al., 2006a; Zhou et al., 2006b;Wu et al., 2006a,b; Zhou et al., 2007; Li et al., 2007a; Munteanu and Yao, 2007; Zhang et al., 2008). Three competing models have been proposed. (1) Li et al. (1999, 2002a, 2003) attributed the extensive Neoproterozoic magmatism in South China to a mantle plume associated with the break-up of Rodinia supercontinent. (2) Zheng et al. (2007, 2008) proposed a plate-rift model that assumes the Neoproterozoic magmatism resulted from lithospheric extension in response to the tectonic evolution from super-continental rift to breakup. (3) Zhou et al. (2002) suggested that the magmatism was associated with two major arcs around the Yangtze Block: the Jiangnan arc to the east and the Hannan–Panxi arc to the west (Zhou et al., 2002, 2006a,b, 2007). To strengthen their arguments, Zhou and co-workers (Zhou et al., 2006a; Zhao and Zhou, 2007) used adakitic rocks occurring in Xuelongbao (750 Ma) and Datian (760 Ma), along the western margin of the Yangtze Craton, as supporting evidence. They interpreted these adakitic rocks as products of partial melting of a subducted oceanic slab. This interpretation, however, has been questioned by Li et al. (2007a) who instead argued for an intra-plate origin. Given these controversies, additional studies are needed to decipher the petrogenesis of the Neoproterozoic adakitic rocks in the western Yangtze Craton.

In this paper, we report geochronological and geochemical data on an adakitic complex in Mopanshan along the western margin of the Yangtze Craton (Fig. 1). New zircon U–Pb isotopic dating reveals

* Corresponding authors.
E-mail addresses: xlhuang@gig.ac.cn (X.-L. Huang), yigangxu@gig.ac.cn (Y.-G. Xu).

0024-4937/$ – see front matter © 2009 Elsevier B.V. All rights reserved.
doi:10.1016/j.lithos.2009.03.028

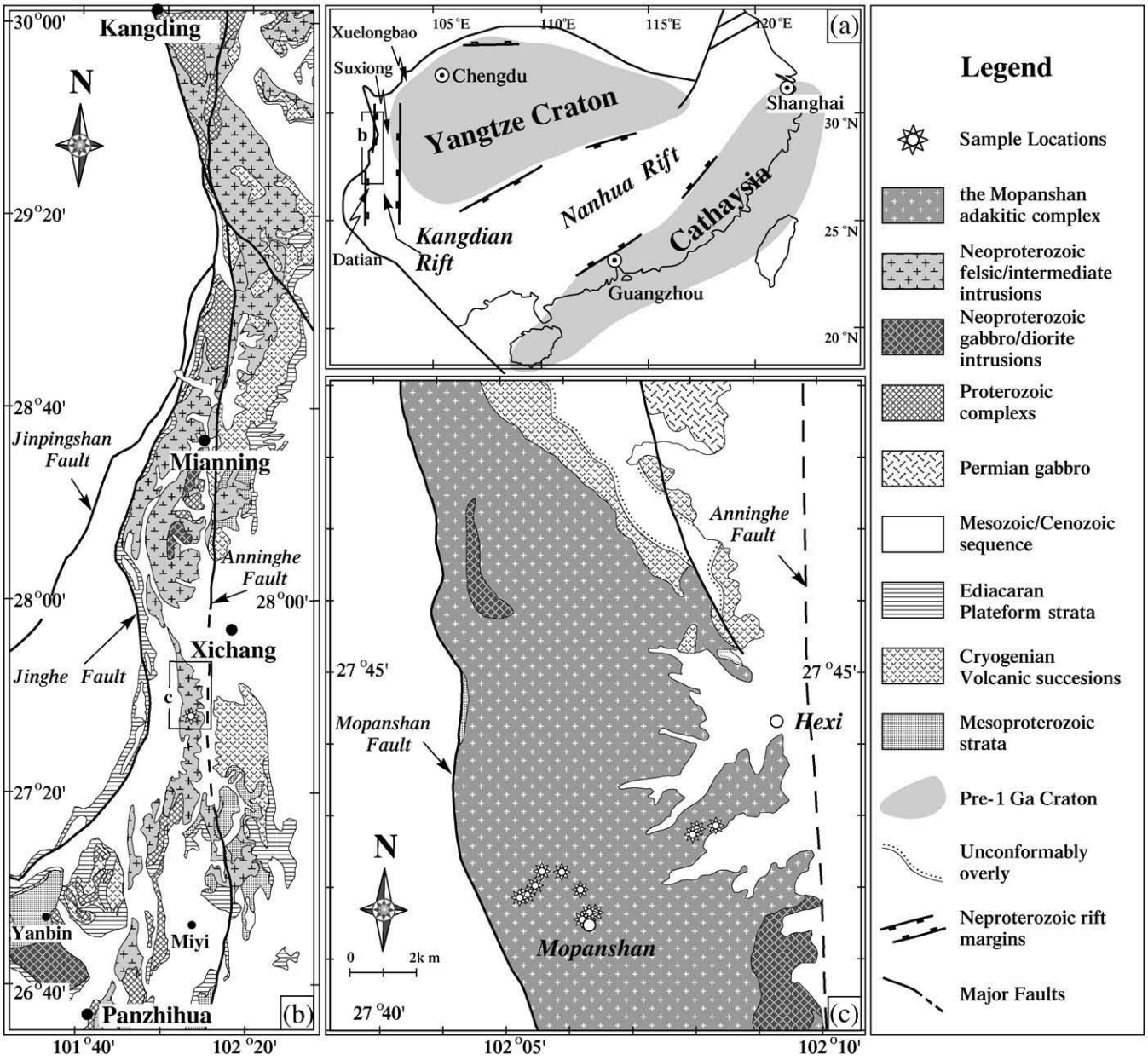

Fig. 1. (a) Neoproterozoic tectonic framework of South China emphasizing two continental rift systems (after Li et al., 1999); (b) Simplified geological map of the North Kangdian area, western South China, illustrating the distribution of Neoproterozoic intrusions, Proterozoic complexes, Mesoproterozoic strata, the Cryogenian successions and the Ediacaran sediments; (c) geological map of the Mopanshan area. Modified after the geological maps in scale of 1/50,000 and Magmatic Rock Map of Sichuan Province (SBGMR, 1991).

that the Mopanshan adakitic complex was emplaced at ~780 Ma, making it contemporaneous with the Mianning A-type granites to the north (Fig. 1). Negative $\varepsilon_{Nd}(t)$ values, the presence of relict zircons and Mesoproterozoic Hf model ages are inconsistent with a derivation from an oceanic slab. More likely, the Mopanshan adakitic rocks were formed by partial melting of a thickened lower crust in an intra-continental rift setting.

2. Geological background and samples

Geologically South China consists of two major blocks, the Yangtze block in the northwest and the Cathaysia block in the southeast (Fig. 1a). The N–S trending Kangdian rift along the western margin of Yangtze Block consists of a Proterozoic sequence including metamorphic complexes, Mesoproterozoic sedimentary strata metamorphosed to greenschist facies (SBGMR, 1991), Neoproterozoic volcanic successions (Cryogenian volcanic successions) and Neoproterozoic sedimentary strata (Ediacaran platform strata). The metamorphic complexes, such as the Kangding and Miyi complexes (Fig. 1b), consist of granitic gneisses that were metamorphosed to upper greenschist to amphibolite metamorphic facies, which have previously been interpreted as the Paleoproterozoic or Archean basement (He et al., 1988; SBGMR, 1991). However, recent geochronological studies indicate that these rocks were most likely formed during the Neoproterozoic (Zhou et al., 2002; Li et al., 2002b). The Suxiong bimodal volcanic rocks of 803 ± 12 Ma (Li et al., 2002a) constitute the most important part of the Cryogenian in the northern part of the Kangdian rift (Liu, 1991; Li et al., 2002a), which overly unconformably Mesoproterozoic metamorphic basement slates (Fig. 1). Cryogenian volcanic successions are conformably overlain by a thick sequence of Ediacaran to Permian strata comprising glacial deposits and clastic, carbonate, and meta-volcanic rocks (Fig. 1) (SBGMR, 1991).

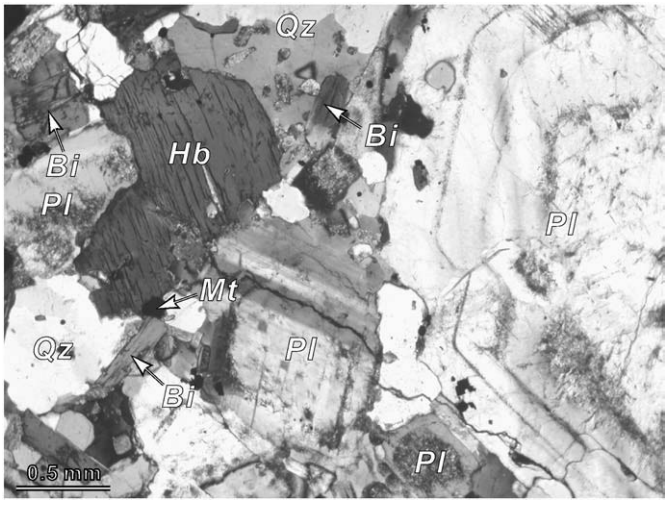

Fig. 2. Petrographic characteristics of the Mopanshan adakitic rocks. Plagioclase (Pl) is the most abundant mineral in the rock, followed by hornblende (Hb), quartz (Qz) and biotite (Bi); most plagioclases are zoned, and large plagioclase phenocrysts show euhedral growth zoning.

The Mopanshan adakitic complex crops out to the east of the *NS*-trending Mopanshan fault and to the west of the Anninghe fault (Fig. 1b). It intruded the Neoproterozoic Suxiong bimodal volcanic successions (803 ± 12 Ma; Li et al., 2002a), Cryogenian diorite intrusions and Mesoproterozoic strata (Fig. 1c). The Mopanshan complex is composed of different intrusive rocks, including tonalite, granodiorite, monzogranite and quartz diorite. There is no obvious connection between tonalite, granodiorite and monzogranite in the field. There is a gradual change from tonalite and granodiorite in the core to monzogranite at margin of the intrusion.

The adakitic samples are all tonalite or granodiorite, and are characterized by equigranular or prophyritic texture (Fig. 2). They are constituted by dominant plagioclase (~65–75%), subordinate hornblende (~5–10%), quartz (~5–25%) and biotite (~5–15%) (Fig. 2). Titanite, epidote and magnetite are the main accessory minerals (<1%). Plagioclase is subhedral tabular with irregular compositional zoning (e.g., An_{25-47}; Fig. 2). Large tabular plagioclase is euhedral with regular zoning (Fig. 2). Hornblende is Mg-rich (~13 wt.% MgO, ~16 wt.% FeOT, ~10 wt.% CaO, ~1 wt.% TiO_2 and <2 wt.% $Na_2O + K_2O$), and biotite is also Mg-rich (~11.5 wt.% MgO and ~20 wt.% FeOT). Both hornblende and biotite are subhedral (Fig. 2), and co-precipitated with plagioclase. Anhedral quartz grains are interstitial to plagioclase, hornblende or biotite (Fig. 2).

3. Analytical methods

Geochemical and Sr–Nd isotopic analyses were carried out at the Guangzhou Institute of Geochemistry, Chinese Academy of Sciences (GIG-CAS). Major element oxides were determined by standard X-ray fluorescence (XRF). Samples were prepared as glass discs using a Rigaku desktop fusion machine. Analyses were performed on a Rigaku ZSX100e instrument at GIG-CAS following the procedure of Li et al. (2006b). Analytical uncertainties are mostly between 1% and 5%. Trace elements were analyzed by inductively coupled plasma-mass spectrometry (ICP-MS) following the procedure of Li (1997). Precision for REE and other incompatible elements is estimated to be better than 5% on the basis of repeated analysis of USGS reference rock standard BIR-1 and laboratory standard (ROA-1). Within-run analytical precision for Nd is better than 2.5% RSD (relative standard deviation). The Sm/Nd ratios measured by ICP-MS are within 2% uncertainty (Li et al., 2002a), and calculation of $\varepsilon_{Nd}(t)$ values for samples of the present study using these Sm/Nd ratios results in uncertainties less than 0.25 units, which is negligible for petrogenetic discussion. Sr and Nd isotopic analyses were performed on a Micromass Isoprobe multi-collector ICPMS, using analytical procedures of Wei et al. (2002) and Li et al. (2004b). Sr and REE were separated using cation columns, and Nd fractions were further separated by HDEHP-coated Kef columns. Measured $^{87}Sr/^{86}Sr$ and $^{143}Nd/^{144}Nd$ ratios were normalized to $^{86}Sr/^{88}Sr = 0.1194$ and $^{146}Nd/^{144}Nd = 0.7219$, respectively. The reported $^{87}Sr/^{86}Sr$ and $^{143}Nd/^{144}Nd$ ratios were adjusted to NBS SRM 987 standard $^{87}Sr/^{86}Sr = 0.71025$ and the Shin Etsu JNdi-1 standard $^{143}Nd/^{144}Nd = 0.512115$, respectively.

Zircons were separated using conventional heavy liquid and magnetic techniques and purified by hand-picking under a binocular microscope. They were mounted together with the standard zircons (TEMORA) in epoxy resin. The mount was polished to ensure grain exposure before gold-coating. The internal structure of zircons was examined using cathodoluminescence (CL) prior to U–Pb isotopic analyses. Zircon U–Pb analyses were performed mainly using a Sensitive High-Resolution Ion Microprobe (SHRIMP II) at the Beijing SHRIMP Center (the Institute of Geology, Chinese Academy of Geological Sciences, Beijing). The analytical procedures are similar to those described by Williams (1998). The standard TEMORA zircon (age 417 Ma) of RSES was used for correction of inter-element fractionation and U, Th and Pb concentrations were determined based on the standard Sri Lankan gem zircon SL13, which has a U concentration of 238 ppm and an age of 572 Ma. Squid (ver. 1.04) and Isoplot (ver. 3.23)

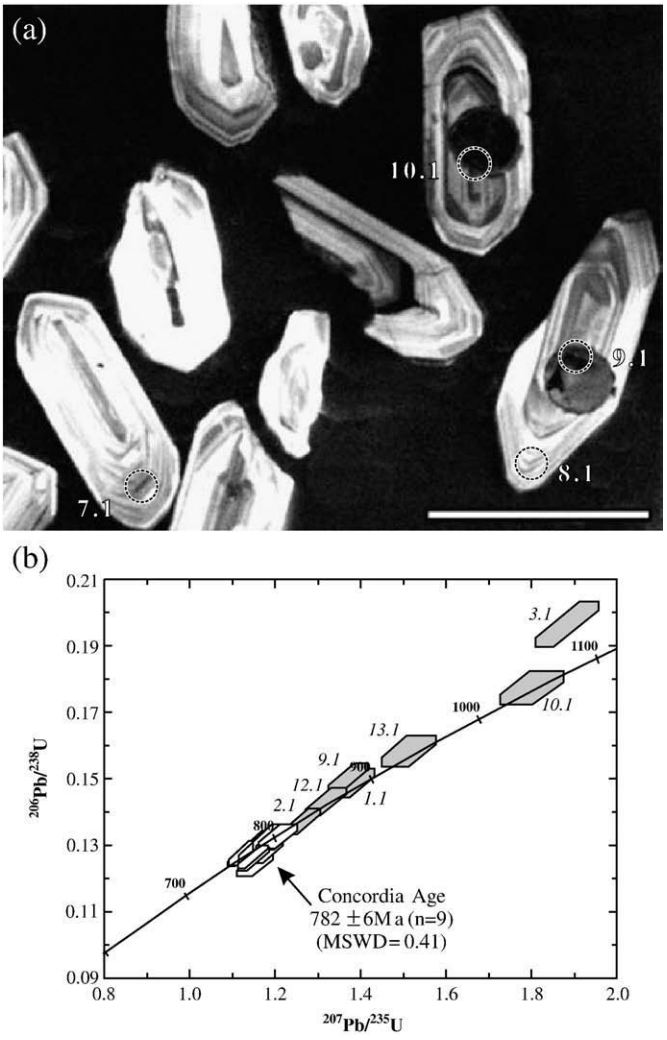

Fig. 3. (a) Representative CL images of zircons; the circles denote locations for SHRIMP U–Pb dating; the length of scale bar is 100 μm; (b) Concordia diagrams of SHRIMP U–Pb zircon dating results for the Mopanshan adakitic rock (MPS05-3).

Table 1
SHRIMP U–Pb zircon data for the Mopanshan adakitic rock.

Spots	U (ppm)	Th (ppm)	Th/U	^{206}Pb (ppm)	f_{206} (%)	^{207}Pb/^{235}U (1σ)	^{206}Pb/^{238}U (1σ)	^{207}Pb/^{206}Pb (1σ)	^{206}Pb/^{238}U Age (Ma)	^{207}Pb/^{206}Pb Age (Ma)
1.1	262	167	0.66	33.4	0.14	1.384 ± 50	0.1486 ± 42	0.0676 ± 14	893 ± 24	855 ± 44
2.1	409	369	0.93	48.3	0.24	1.264 ± 42	0.1372 ± 38	0.0668 ± 12	829 ± 22	832 ± 37
3.1	305	193	0.66	51.6	0.13	1.883 ± 73	0.1965 ± 67	0.0695 ± 13	1157 ± 36	913 ± 38
4.1	441	334	0.78	48.4	0.06	1.128 ± 37	0.1277 ± 36	0.0641 ± 12	775 ± 20	744 ± 39
5.1	232	204	0.91	25.8	0.53	1.166 ± 52	0.1286 ± 37	0.0658 ± 22	780 ± 21	800 ± 71
6.1	371	345	0.96	41.2	0.10	1.139 ± 50	0.1290 ± 53	0.0640 ± 9	782 ± 31	743 ± 29
7.1	346	322	0.96	39.3	0.14	1.193 ± 38	0.1319 ± 37	0.0656 ± 10	799 ± 21	794 ± 31
8.1	440	355	0.83	47.7	0.15	1.149 ± 36	0.1258 ± 35	0.0662 ± 10	764 ± 20	814 ± 31
9.1	202	148	0.76	26.1	0.12	1.371 ± 45	0.1504 ± 42	0.0661 ± 11	903 ± 24	810 ± 36
10.1	257	175	0.71	39.1	0.16	1.801 ± 76	0.1772 ± 50	0.0737 ± 23	1051 ± 27	1034 ± 62
11.1	279	269	1.00	31.9	0.22	1.207 ± 45	0.1327 ± 37	0.0660 ± 16	803 ± 21	805 ± 50
12.1	214	209	1.01	26.3	0.13	1.319 ± 47	0.1431 ± 43	0.0669 ± 13	862 ± 24	834 ± 43
13.1	396	428	1.12	54.0	0.12	1.512 ± 64	0.1584 ± 46	0.0692 ± 21	948 ± 26	906 ± 63
14.1	198	163	0.85	21.1	0.18	1.153 ± 43	0.1241 ± 35	0.0674 ± 16	754 ± 20	851 ± 48
15.1	314	341	1.12	35.8	0.09	1.197 ± 49	0.1325 ± 37	0.0655 ± 20	802 ± 21	791 ± 63
16.1	376	535	1.47	40.9	0.09	1.148 ± 34	0.1266 ± 35	0.0658 ± 8	768 ± 20	800 ± 25

programs were used for raw data reduction and age calculation, and the ^{204}Pb-based method of common Pb correction was applied. Uncertainties reported in Table 1 are all ±1σ. The ages quoted in the text (either ^{207}Pb/^{206}Pb ages or ^{206}Pb/^{238}U ages) are the weighted mean at the 95% confidence level.

In-situ zircon Hf isotopic analyses were carried out on the dated spots using a Neptune MC-ICPMS, equipped with a 193 nm laser, at the Institute of Geology and Geophysics, Chinese Academy of Sciences in Beijing. Spot sizes of 40 μm with a laser repetition rate of 8 Hz at 100 mJ were used. The detailed analytical technique and data correction procedure are described in Xu et al. (2004) and Wu et al. (2006a,b). During analysis, ^{176}Hf/^{177}Hf and ^{176}Lu/^{177}Hf ratios of the standard zircon (91500) were 0.282292 ± 14 (2σ) and 0.00029, similar to the ^{176}Hf/^{177}Hf ratios of 0.282284 ± 22 measured using the laser method (Griffin et al., 2006) and the ^{176}Hf/^{177}Hf ratios of 0.282302 ± 8 measured using the solution method (Wiedenbeck et al., 2004).

4. Results

4.1. Zircon U–Pb geochronology and Hf isotopes

Zircon grains of MPS05-3 separated for SHRIMP U–Pb dating and LA-ICPMS Lu–Hf isotopes analyses display well-developed prismatic dipyramids. Cathodoluminescence (CL) images show oscillatory zonings in these zircons (Fig. 3a), pointing to a magmatic origin. Some zircons have distinctive cores (Fig. 3a), which may be inherited from previous events. All these inherited cores must also be of magmatic origin given their oscillatory zonings.

Most SHRIMP U–Pb dating analyses are concordant but show variable ^{206}Pb/^{238}U ages (Fig. 3b; Table 1). A concordant age of 782 ± 6 Ma (MSWD = 0.41) based on the nine youngest analyses is interpreted as the emplacement age (Fig. 3b; Table 1). Six concordant analyses of inherited cores yield ^{206}Pb/^{238}U ages of 829–1051 Ma. One reverse discordant analysis (Spot 3.1) has a ^{206}Pb/^{238}U age of 1157 ± 36 Ma and a ^{207}Pb/^{206}Pb age of 913 ± 38 Ma.

Eighteen Lu–Hf analyses have been done on zircons from MPS05-3, most of which have been dated by SHRIMP U–Pb methods on the same analytical spots (Table 2). The initial Hf isotope ratios are calculated at 780 Ma. As a whole, the inherited zircons have relatively high single-stage Hf model ages (1192 to 1273 Ma with a weighted mean of 1234 ± 33 Ma; Table 2). The $\varepsilon_{Hf}(t)$ values of the relict zircons are low when calculated for an age of 780 Ma (1.91 ± 1.18 to 3.83 ± 1.01; Table 2), but ε_{Hf} (t_r) values are high when calculated using their ^{206}Pb/^{238}U ages (4.33 ± 1.18 to 10.16 ± 1.28; Table 2). Other zircon $\varepsilon_{Hf}(t)$ values vary from 4.23 to 7.07 with a weighted mean of 5.43 ± 0.65, which is lower than that of the contemporary Mianning A-type

Table 2
LA-MC-ICPMS zircon Lu–Hf isotope data for the Mopanshan adakitic rock.

Spots	^{176}Yb/^{177}Hf	^{176}Lu/^{177}Hf	^{176}Hf/^{177}Hf (±2σ)	ε_{Hf} (t)	(±2σ)	ε_{Hf} (t_r)	(±2σ)	T_{DM} (Ma)	(±2σ)	SHRIMP Spots	^{206}Pb/^{238}U Age (Ma)
01	0.028955	0.001136	0.282457 ± 24	5.49	0.86			1129	34	14.1	754 ± 20
02	0.033300	0.001330	0.282360 ± 28	1.97	0.98	5.56	0.86	1271	39	13.1*	948 ± 26
03	0.024540	0.001004	0.282432 ± 29	4.68	1.03			1160	41		
04	0.025665	0.001043	0.282494 ± 31	6.86	1.11			1074	44		
05	0.025339	0.001029	0.282421 ± 26	4.28	0.93			1176	37		
06	0.020589	0.000830	0.282406 ± 29	3.83	1.01	5.61	1.01	1192	40	12.1*	862 ± 24
07	0.014710	0.000598	0.282396 ± 23	3.60	0.83	4.67	0.83	1198	32	2.1*	829 ± 22
08	0.028494	0.001126	0.282361 ± 24	2.10	0.84	4.75	0.84	1263	33	9.1*	903 ± 24
09	0.033790	0.001255	0.282358 ± 33	1.91	1.18	4.33	1.18	1273	47	1.1*	893 ± 24
10	0.019243	0.000777	0.282472 ± 26	6.20	0.94			1098	37		
11	0.026748	0.001077	0.282394 ± 21	3.30	0.74	9.15	0.74	1215	29	10.1*	1051 ± 27
12	0.029160	0.001202	0.282460 ± 34	5.54	1.21			1127	48		
13	0.023745	0.000943	0.282419 ± 33	4.23	1.15			1177	46	6.1	782 ± 31
14	0.024720	0.000997	0.282356 ± 36	1.98	1.28	10.16	1.28	1267	50	3.1*	1157 ± 36
15	0.028206	0.001105	0.282456 ± 37	5.46	1.32			1130	52	5.1	780 ± 21
16	0.021933	0.000903	0.282498 ± 31	7.07	1.11			1064	44	4.1	775 ± 20
17	0.017972	0.000740	0.282464 ± 43	5.95	1.52			1107	60	16.1	768 ± 20
18	0.034285	0.001392	0.282437 ± 25	4.63	0.89			1166	36		

Notes: (1) the superscript * denotes the SHRIMP Spots on inherited zircons. (2) Initial Hf isotope ratios are calculated with the reference to the chondritic reservoir at the time of magma crystallization, a decay constant for ^{176}Lu of 1.865 × 10^{-11} yr^{-1} and the chondritic ratios of ^{176}Hf/^{177}Hf (= 0.282772) and ^{176}Lu/^{177}Hf (= 0.0332) (Blichert-Toft and Albarede, 1997) were adopted. Single-stage model ages (T_{DM}) are calculated using the measured ^{176}Lu/^{177}Hf ratios, referred to a model depleted mantle with a present-day ^{176}Hf/^{177}Hf ratio of 0.28325 and ^{176}Lu/^{177}Hf = 0.0384 (Griffin et al., 2000). t = 780 Ma, t_r are ^{206}Pb/^{238}U ages of relict zircons.

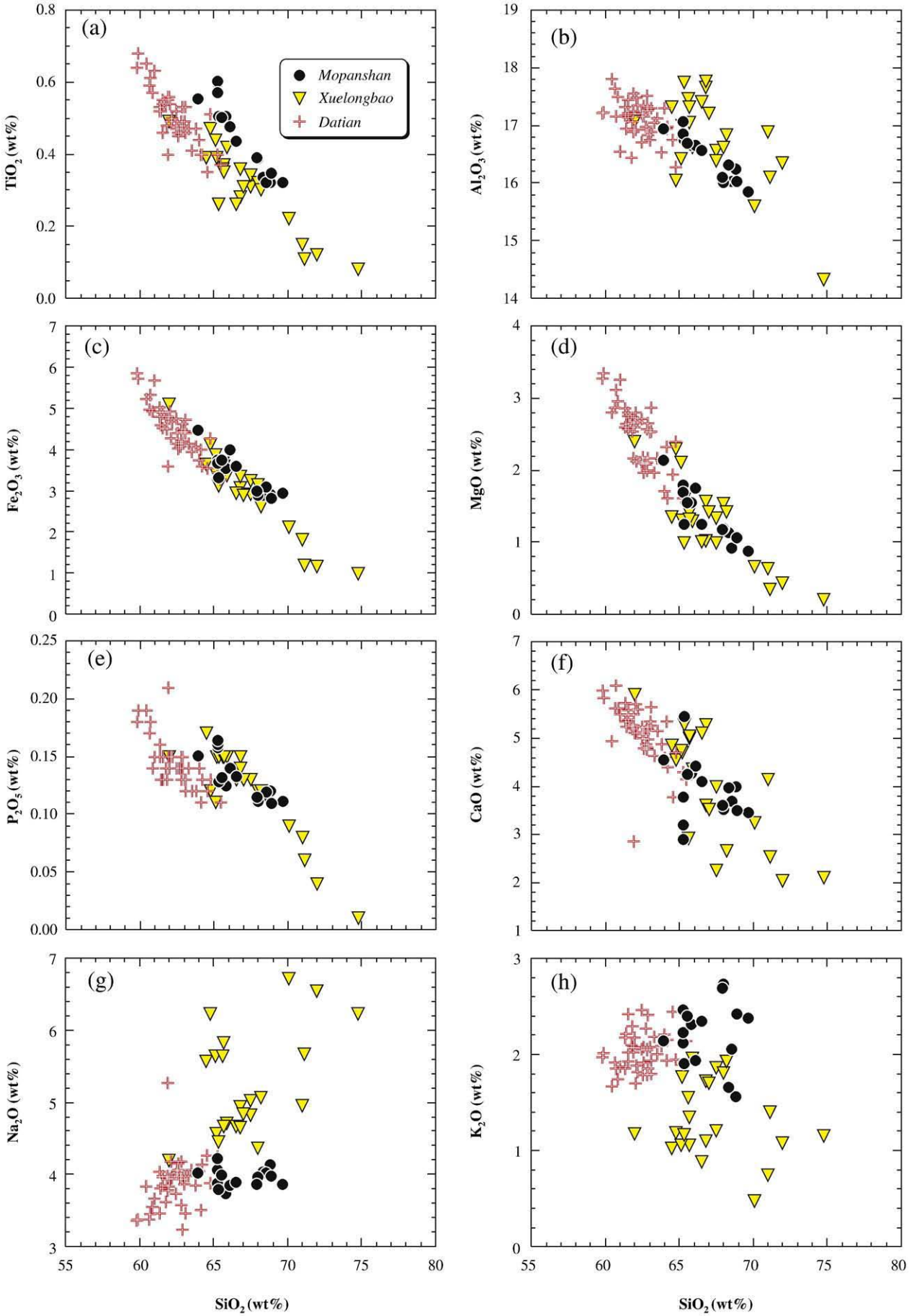

Fig. 4. Variations of some major elements with SiO_2 for the Mopanshan adakitic rocks. Data for Xueolongbao and Datian are from Zhou et al. (2006a) and Zhao and Zhou (2007).

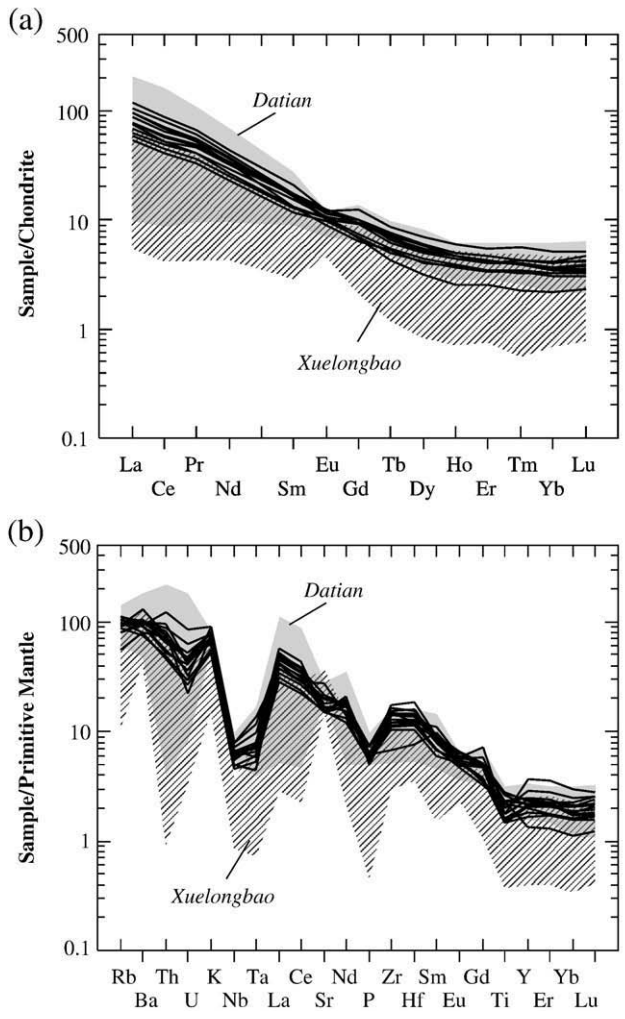

Fig. 5. Chondrite-normalized REE patterns and primitive mantle-normalized trace element spidergrams of the Mopanshan adakitic rocks. The adakites from Xueolongbao (Zhou et al., 2006a) and Datian (Zhao and Zhou, 2007) are also shown for comparison. Chondrite and PM normalization factors from Taylor and McLennan (1985) and Sun and McDonough (1989), respectively.

granites (weighted mean 10.7 ± 0.4; Huang et al., 2008) and higher than that of the ~825 Ma granitoids from western part of the Jiangnan orogen in South China (−3.4 ± 0.8 to −1.6 ± 0.8; Zheng et al., 2007), but are similar to the ~750 Ma bimodal intrusives in South China (3.5 ± 0.8 to 9.9 ± 0.8; Zheng et al., 2007; Zhao et al., 2008; Zheng et al., 2009) and the ~825 Ma granitoids in the eastern part of the Jiangnan orogen in South China (3.4 ± 1.6 to 5.4 ± 2.7; Wu et al., 2006a,b; Zheng et al., 2008). Single-stage Hf model ages for these youngest zircons range from 1064 to 1177 Ma with a weighted mean of 1131 ± 26 Ma (Table 2), distinctively older than those of the Mianning A-type granite (weighted mean 933 ± 16 Ma; Huang et al., 2008), but similar to the ~750 Ma bimodal intrusives in the Kangdian Rift (weighted mean 1.07 ± 0.11 Ga; Zheng et al., 2007) and the northern margin of the Yangtze Craton (Zhao et al., 2008; Zheng et al., 2009). Essentially, the Lu–Hf isotope composition of zircons in this study overlaps that reported by Zheng et al. (2007) for the same region within the data range of zircons from South Anhui and Dabie–Sulu (Wu et al., 2006a,b; Zhao et al., 2008; Zheng et al., 2008, 2009).

4.2. Major and trace elements

The Mopanshan adakitic rocks have medium SiO_2 (63.92–69.69 wt.%) and K_2O contents (0.56–2.73 wt.%) but relatively high Al_2O_3 (15.84–17.07 wt.%), CaO (2.89–5.45 wt.%), Na_2O (3.73–4.22 wt.%) contents and Na_2O/K_2O ratios (1.43–2.65). They have relatively low Fe_2O_3 (2.81–4.47 wt.%), MgO (0.88–2.14 wt.%) and TiO_2 (0.32–0.60 wt.%). Contents of TiO_2, Al_2O_3, Fe_2O_3, MgO, P_2O_5 and CaO in the Mopanshan adakitic rocks decrease with increasing SiO_2 (Fig. 4a–f). Similar correlations have been observed in adakites from Xuelongbao and Datian (Zhou et al., 2006a; Zhao and Zhou, 2007). Neither Na_2O nor K_2O correlates with SiO_2 (Fig. 4g–h). The Mopanshan samples show LREE-enriched and HREE-depleted patterns ($(La/Yb)_N$ = 12–44, Yb_N = 2.2–5.9) with weak Eu anomalies (Eu/Eu* = 0.65–1.12) (Fig. 5a). They contain moderate Sr (311–577 ppm) but very low Y (6.06–16.6 ppm) and Yb contents (0.54–1.46 ppm). On the primitive mantle-normalized spidergram, the Mopanshan samples are characterized by enrichment of LILEs such as Rb, Ba, Th, U, K and LREE and pronounced negative Nb–Ta, P and Ti anomalies (Fig. 5b).

Most of the Mopanshan samples plot in the field of adakite and high Al-TTG on $(La/Yb)_N$ versus Yb_N and Sr/Y versus Y diagrams (Fig. 6). These are adakitic rocks, but not TTGs, because most of the samples have medium SiO_2 (63.92–69.69 wt.%), ferromagnesian contents (Fe_2O_3 + MgO + MnO + TiO_2 = 4.19–7.23 wt.%; Mean = 5.28) and K_2O contents (0.56–2.73 wt.%) with relatively high K_2O/Na_2O ratios (0.38–0.70; Mean = 0.56), which are distinctively different from the typical TTG (Martin et al., 2005). One sample (MPS06-9) plotted out of the adakite field with a low Sr/Y ratio but a high Y content (Table 3; Fig. 6b). This sample may have been subjected to fractional crystallization of

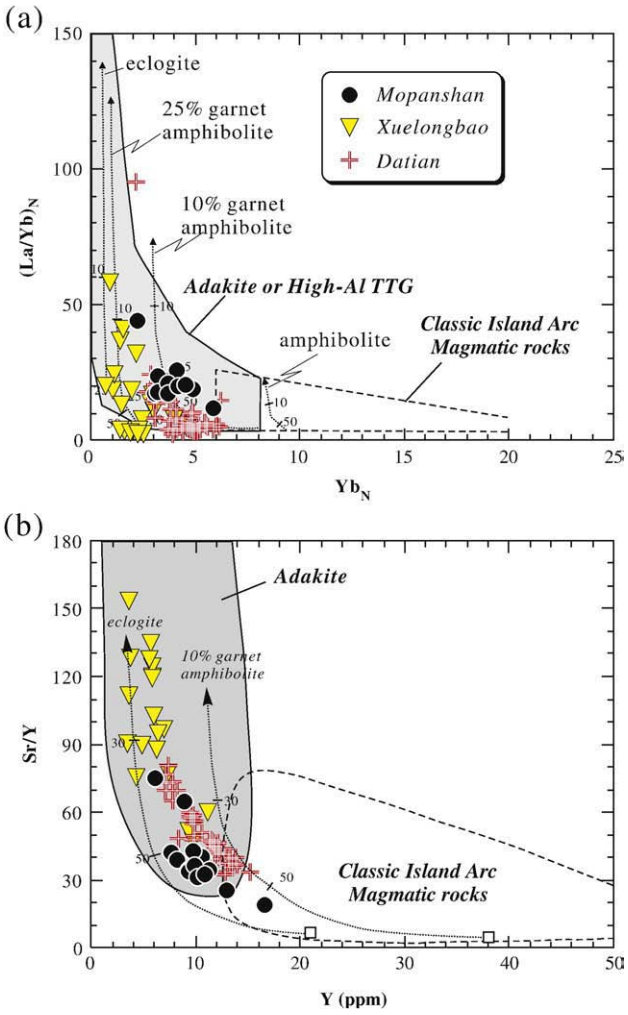

Fig. 6. Plots of $(La/Yb)_N$ vs. Yb_N and Sr/Y vs. Y for the Mopanshan adakitic rocks. Fields of adakites, and classic island arc magmatic rocks are from Defant and Drummond (1990) and Martin et al. (2005). Partial melting curves for basalt leaving residues of eclogite, garnet amphibolite and amphibolite from Drummond and Defant (1990). Data for Xueolongbao and Datian are from Zhou et al. (2006a) and Zhao and Zhou (2007).

Table 3
Major (wt.%) and trace element (ppm) data for the Mopanshan adakitic rock.

Sample	MPS 05-1	MPS 05-2	MPS 05-3	MPS 05-5	MPS 05-6	MPS 06-5	MPS 06-6	MPS 06-14	MPS 06-15	MPS 06-16	MPS 06-17	MPS 06-19	MPS 06-8	MPS 06-9	MPS 06-10	MPS 06-11
SiO_2	65.26	65.24	65.83	65.33	66.07	65.23	65.55	68.86	68.34	68.55	68.86	63.92	67.97	67.92	69.69	66.51
TiO_2	0.60	0.60	0.51	0.51	0.48	0.57	0.50	0.32	0.34	0.32	0.35	0.55	0.39	0.39	0.32	0.44
Al_2O_3	17.06	17.07	16.65	16.75	16.65	16.84	16.69	16.25	16.32	16.03	16.03	16.94	16.02	16.09	15.84	16.57
Fe_2O_3	3.74	3.73	3.54	3.32	3.98	3.67	3.75	2.90	2.88	3.09	2.81	4.47	2.88	2.99	2.93	3.59
MnO	0.06	0.05	0.05	0.05	0.05	0.05	0.06	0.05	0.11	0.05	0.06	0.07	0.06	0.05	0.06	0.05
MgO	1.75	1.79	1.55	1.24	1.75	1.69	1.55	1.08	1.13	0.92	1.06	2.14	1.19	1.18	0.88	1.25
CaO	3.78	3.20	4.27	5.45	4.41	2.89	4.24	4.00	3.98	3.69	3.49	4.54	3.52	3.60	3.45	4.09
Na_2O	3.87	4.07	3.73	3.79	3.85	4.22	4.00	4.13	4.04	4.02	3.97	4.03	3.96	3.86	3.86	3.89
K_2O	2.12	2.23	2.31	1.90	1.93	2.47	2.40	1.56	1.66	2.06	2.42	2.14	2.73	2.69	2.37	2.34
P_2O_5	0.16	0.16	0.13	0.13	0.14	0.16	0.13	0.12	0.12	0.12	0.11	0.15	0.11	0.12	0.11	0.13
LOI	1.56	1.88	0.85	1.51	0.99	1.87	0.96	0.71	0.71	0.50	1.06	1.55	1.29	0.78	0.61	0.60
Total	99.95	100.02	99.42	99.97	97.37	99.67	99.83	99.97	99.61	99.33	100.20	100.49	100.12	99.67	100.12	99.46
Mg#	48.1	48.7	46.4	42.6	46.5	47.7	45.0	42.4	43.8	37.0	42.8	48.4	45.1	44.0	37.2	41.0
A/CNK	1.10	1.14	1.01	0.92	1.01	1.13	0.99	1.03	1.04	1.03	1.03	0.99	1.01	1.02	1.04	1.01
Cr	21.0	15.8	15.9	16.5	31.1	13.7	22.9	10.8	8.99	6.27	8.02	27.3	22.7	19.0	5.21	11.9
Ni	7.65	6.02	4.87	5.56	11.6	4.37	11.5	3.41	3.12	1.64	1.69	11.0	8.01	5.08	2.20	3.63
Ga	19.8	20.5	20.8	20.0	19.6	19.9	19.3	18.3	19.9	19.2	18.7	21.6	19.1	18.4	18.3	20.6
Rb	50.8	61.6	70.8	63.5	66.0	57.3	58.4	35.7	56.0	51.3	50.3	57.2	71.5	68.2	59.8	64.4
Ba	652	651	693	553	624	745	736	562	525	693	688	703	651	719	920	714
Sr	422	422	383	454	577	419	362	322	319	319	316	482	348	311	314	325
Y	10.8	10.6	11.3	6.06	8.96	9.79	9.93	7.64	8.18	9.33	9.34	12.8	10.8	16.6	10.1	13.0
Zr	161	163	195	143	165	184	166	117	123	128	135	133	172	136	157	75.9
Hf	4.38	4.53	5.76	3.93	3.72	4.81	4.28	3.22	3.46	3.63	3.98	3.83	4.93	3.68	4.22	2.33
Nb	4.72	4.53	4.53	3.56	4.80	4.46	4.34	3.21	3.40	4.01	3.94	5.11	5.62	5.58	4.33	5.11
Ta	0.33	0.29	0.32	0.18	0.24	0.31	0.29	0.22	0.25	0.31	0.32	0.38	0.48	0.57	0.27	0.40
Pb	10.4	8.62	10.2	7.02	12.3	11.5	10.1	5.3	5.6	10.9	10.6	15.1	14.4	11.4	12.4	11.1
Th	4.65	4.41	6.01	6.18	5.87	5.74	5.51	3.90	4.15	7.05	8.12	9.79	10.3	6.46	6.47	7.46
U	0.76	0.85	1.10	0.98	0.98	0.97	0.99	0.57	0.62	0.88	0.91	1.34	1.78	0.68	0.47	1.30
La	28.9	25.4	32.3	35.4	27.8	28.5	23.1	19.5	21.4	35.3	39.1	44.1	33.8	25.8	30.4	34.2
Ce	55.3	50.7	62.2	65.5	50.4	56.6	47.2	39.3	42.4	68.6	76.3	84.6	65.6	52.1	60.0	67.4
Pr	6.58	6.27	7.38	7.25	5.59	6.70	5.64	4.57	5.00	7.66	8.41	9.17	7.24	6.30	6.64	7.63
Nd	24.0	22.8	25.8	23.6	19.0	24.2	20.9	16.5	17.9	26.2	28.5	30.8	24.3	23.8	22.8	26.9
Sm	3.95	3.85	4.05	3.03	3.05	4.03	3.60	2.69	3.01	3.82	4.06	4.77	3.66	4.95	3.53	4.33
Eu	1.02	1.07	0.99	0.91	0.78	1.10	0.92	0.85	0.89	0.88	0.89	1.04	0.82	0.98	0.83	0.96
Gd	3.07	3.04	3.07	2.04	1.92	3.11	2.89	2.17	2.29	2.83	3.08	3.87	2.96	4.26	2.77	3.45
Tb	0.43	0.41	0.44	0.25	0.31	0.40	0.40	0.29	0.32	0.36	0.38	0.50	0.37	0.67	0.37	0.48
Dy	2.22	2.18	2.29	1.20	1.51	2.04	2.05	1.58	1.71	1.89	1.95	2.65	2.02	3.61	2.01	2.57
Ho	0.40	0.40	0.43	0.22	0.32	0.40	0.40	0.32	0.33	0.38	0.40	0.52	0.40	0.70	0.41	0.51
Er	1.08	1.05	1.16	0.63	0.85	1.00	1.01	0.83	0.85	1.00	1.00	1.35	1.09	1.72	1.07	1.33
Tm	0.14	0.14	0.15	0.08	0.12	0.14	0.14	0.12	0.13	0.15	0.15	0.20	0.17	0.25	0.16	0.20
Yb	0.87	0.85	1.02	0.54	0.80	0.92	0.91	0.76	0.80	1.01	1.02	1.29	1.13	1.46	1.03	1.21
Lu	0.13	0.13	0.16	0.09	0.13	0.14	0.15	0.12	0.13	0.16	0.18	0.20	0.19	0.20	0.16	0.19
Eu/Eu*	0.90	0.95	0.86	1.12	0.98	0.95	0.87	1.08	1.04	0.81	0.77	0.74	0.76	0.65	0.81	0.76
La/Yb_N	22.4	20.1	21.5	44.0	23.6	21.0	17.1	17.3	18.0	23.5	25.9	23.0	20.3	12.0	19.9	19.1
Yb_N	3.52	3.44	4.10	2.19	3.21	3.70	3.68	3.07	3.23	4.08	4.12	5.21	4.54	5.88	4.17	4.89
Sr/Y	39.1	39.8	34.0	75.0	64.4	42.8	36.4	42.2	39.1	34.2	33.8	37.7	32.1	18.7	31.1	25.0
Nb/La	0.16	0.18	0.14	0.10	0.17	0.16	0.19	0.16	0.16	0.11	0.10	0.12	0.17	0.22	0.14	0.15
Ti/Yb	4085	4232	2985	5575	3589	3725	3299	2533	2511	1901	2037	2570	2067	1599	1868	2156

Notes: (1) $A/CNK = Al_2O_3/(CaO + Na_2O + K_2O)$ (molar ratio); (2) subscript N = chondrite-normalized value.

plagioclase resulting in low Sr contents and Eu/Eu* values (0.65; Table 3).

4.3. Sr–Nd isotopes

The Mopanshan adakitic rocks have low $^{143}Nd/^{144}Nd$ ratios (0.511527–0.511610) with negative $\varepsilon_{Nd}(t)$ values (−2.06 to −0.43). Their initial $^{87}Sr/^{86}Sr$ ratios range from 0.7043–0.7056 (Table 4). As a whole, the Mopanshan samples have enriched initial $^{87}Sr/^{86}Sr$ ratios and ε_{Nd} values compared to the Xuelongbao and Datian adakitic complex (Zhou et al., 2006a; Zhao and Zhou, 2007) (Fig. 7a). As shown in Fig. 7b, $\varepsilon_{Nd}(t)$ values of these adakitic rocks are distinctively lower than those of the Mianning A-type granites, Yanbian mafic intrusions (800–810 Ma; Zhou et al., 2006b) and basalts (~900 Ma; Li et al., 2006a), Suxiong basaltic rocks (803 ± 12 Ma; Li et al., 2002a), Lengqi gabbros with less crustal contamination (808 ±

Table 4
Sr and Nd isotope compositions of the Mopanshan adakitic rock.

Samples	$^{87}Rb/^{86}Sr$	$^{87}Sr/^{86}Sr$	$(^{87}Sr/^{86}Sr)_i$	$^{147}Sm/^{144}Nd$	$^{143}Nd/^{144}Nd$	$(^{143}Nd/^{144}Nd)_i$	T_{DM} (Ma)	$\varepsilon_{Nd}(t)$
MPS05-1	0.3483	0.708836 ± 14	0.704957	0.0995	0.512113 ± 9	0.511604	1385	−0.54
MPS05-3	0.5350	0.710234 ± 14	0.704275	0.0949	0.512012 ± 10	0.511527	1460	−2.06
MPS05-5	0.4048	0.709956 ± 13	0.705447	0.0776	0.512007 ± 8	0.511610	1281	−0.43
MPS05-6	0.3309	0.709335 ± 17	0.705649	0.0971	0.512030 ± 9	0.511534	1464	−1.92

Notes: (1) $^{87}Rb/^{86}Sr$ and $^{147}Sm/^{144}Nd$ are calculated using whole-rock Rb, Sr, Sm and Nd contents in Table 3; (2) The errors of $^{87}Sr/^{86}Sr$ and $^{143}Nd/^{144}Nd$ are all 2σ; (3) $\varepsilon_{Nd}(t) = [(^{143}Nd/^{144}Nd)_S/(^{143}Nd/^{144}Nd)_{CHUR} - 1] \times 10000$; $T_{DM} = \ln\{[(^{143}Nd/^{144}Nd)_s - (^{143}Nd/^{144}Nd)_{DM}]/[(^{143}Sm/^{144}Nd)_s - (^{147}Sm/^{144}Nd)_{DM}]\}/\lambda$ (DePaolo, 1981); In the calculation, $(^{143}Nd/^{144}Nd)_{CHUR} = 0.512638$, $(^{147}Sm/^{144}Nd)_{CHUR} = 0.1967$, $(^{143}Nd/^{144}Nd)_{DM} = 0.51315$, $(^{147}Sm/^{144}Nd)_{DM} = 0.2136$ and $t = 780$ Ma.

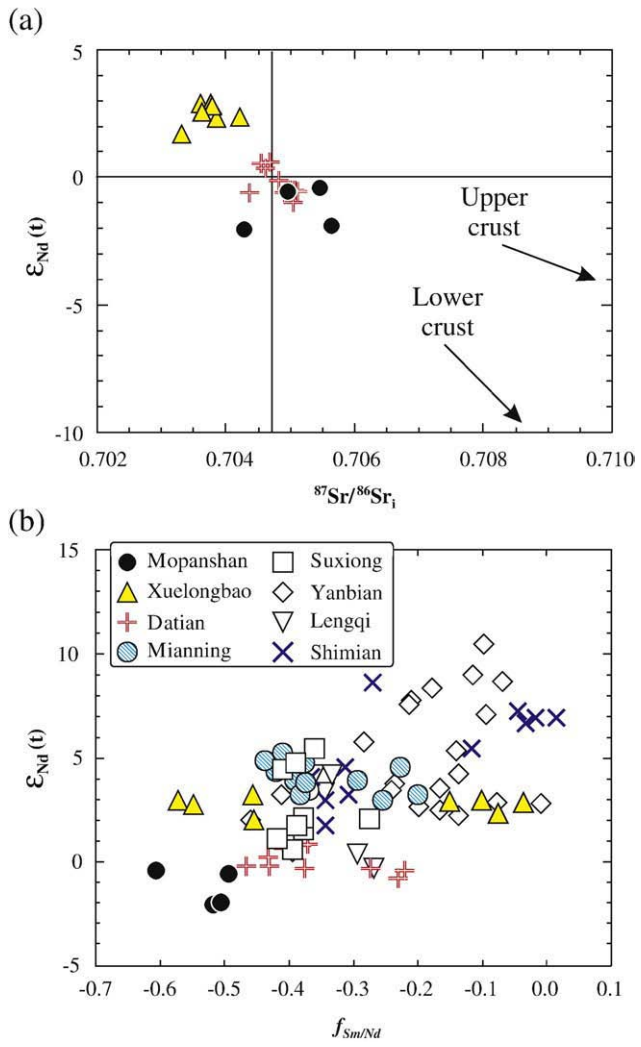

Fig. 7. (a) $\varepsilon_{Nd}(t)$ vs. $(^{87}Sr/^{86}Sr)_i$ and (b) $\varepsilon_{Nd}(t)$ vs. $f_{Sm/Nd}$ diagrams for the Mopanshan adakitic rocks and some Mesoproterozoic to Neoproterozoic mafic intrusions or volcanic rocks at north Kangdian rift. $t = 780$ Ma is used for the calculation of $\varepsilon_{Nd}(t)$ values for all the samples. Data sources: Mianning granites (Huang et al., 2008); Suxiong biomodal volcanic rocks (Li et al., 2002a); Lengqi gabbro (Li et al., 2002c); Yanbian mafic intrusions (Zhou et al., 2006b) and basalts (Li et al., 2006a); Shimian mafic dikes (Lin et al., 2007).

12 Ma; Li et al., 2002c) and Shimian mafic dykes (760–780 Ma; Lin et al., 2007).

5. Discussion

5.1. Petrogenesis

Adakites are generally derived from sources with basaltic compositions (Rapp et al., 1999; Martin et al., 2005; Condie, 2005). Several genetic models have been proposed for the origin of adakites and adakitic rocks (Castillo, 2006; Wang et al., 2006a, and references therein), including crustal assimilation and fractional crystallization (AFC) processes from parental basaltic magmas (Castillo et al., 1999; Castillo, 2006; Macpherson et al., 2006), partial melting of a subducting oceanic slab (Defant and Drummond, 1990; Kay et al., 1993; Drummond et al., 1996; Sajona et al., 2000), partial melting of mafic rocks in the lower part of a thickened crust (Atherton and Petford, 1993; Muir et al., 1995; Petford and Atherton, 1996; Johnson et al., 1997; Xiong et al., 2003; Chung et al., 2003; Hou et al., 2004; Wang et al., 2005, 2006b) and partial melting of a stalled (or dead) slab in the mantle or delaminated lower crust (Xu et al., 2002; Wang et al., 2006a). These models are briefly discussed below.

5.1.1. Fractional crystallization versus partial melting

The major element variations (Fig. 4) suggest that the Mopanshan adakitic rocks have experienced some degree of fractional crystallization during their evolution. Specifically, the decrease in Sr but increase in Ba with decreasing Eu/Eu* (Fig. 8a–b) are indicative of plagioclase fractionation. Fractionation of plagioclase is consistent with the abundant euhedral and normally zoned plagioclase phenocrysts in the samples. Ti-bearing minerals (such as ilmenite, titanite, etc.) might be other fractionated phases given the presence of titanite in some samples and the decreasing TiO_2 with increasing SiO_2 (Fig. 4a). Fractional crystallization of the titanium-rich minerals may be responsible for the negative Nb–Ta and Ti anomalies in the basalts (e.g., Xiong et al., 2005). However, this cannot be the main reason for significant negative Nb–Ta anomalies in the Mopanshan adakitic rocks because of the nearly constant Nb/La ratios (0.10–0.22; Table 3) with respect to variable TiO_2 contents (0.32–0.60 wt.%; Table 3) (Fig. 8c) and Ti/Yb ratios (1599–5575; Table 3). It is likely that negative Nb–Ta anomalies of the Mopanshan adakitic rocks reflect the source characteristics.

Castillo et al. (1999) demonstrated that Sr/Y and La/Yb could increase significantly as a result of fractionation of amphibole and/or garnet at relatively high pressures. Removal of plagioclase and amphibole at low pressure will also lower Dy/Yb of the residual melt (Macpherson et al., 2006). However, the positive (or negative) correlations between Sr/Y (and La/Yb) and MgO or SiO_2, expected by the fractionation model (Castillo et al., 1999; Macpherson et al., 2006) are not observed for the Mopanshan samples (Fig. 8d–e–f). This suggests that the low HREE and high Sr/Y ratios of the Mopanshan rocks were not related to fractionation processes. The fractionation model is not favored also because of the very low proportion of contemporary mafic rocks (Li et al., 2002a) compared to the volume of adakitic rocks in the Kangdian Rift (Fig. 1c).

To make further distinction between the melting model and the fractionation model, we have modeled the variation of Y and Yb contents during fractionation and melting processes. Both amphibole and garnet have much high partition coefficients for Yb than Y in the andesitic system (GERM website: http://earthref.org/GERM/). Thus partial melting and fractionation would yield distinctively different trends in the plot of Y/Yb vs Y (Fig. 9). The fractional crystallization of amphibole or garnet will increase Y/Yb ratios in the residual melts, as exemplified by the Mindanao adakites from the Philippines (Fig. 9, Macpherson et al., 2006). The Mopanshan adakitic rocks have nearly constant Y/Yb ratios (Fig. 9), which is inconsistent with the fractionation model. The variation of Y/Yb in the Mopanshan samples can be explained by partial melting of mafic materials with residual amphibole and garnet in the source (Fig. 9), followed by fractional crystallization of plagioclase (Fig. 9).

5.1.2. Source characteristics of the Mopanshan adakites

The potential sources of adakitic rocks include a subducting oceanic slab (Defant and Drummond, 1990; Kay et al., 1993; Drummond et al., 1996; Sajona et al., 2000), delaminated lower crust (Xu et al., 2002; Wang et al., 2006a) or thickened lower crust (Atherton and Petford, 1993; Muir et al., 1995; Petford and Atherton, 1996; Johnson et al., 1997; Xiong et al., 2003; Chung et al., 2003; Hou et al., 2004; Wang et al., 2005, 2006b). In the first two cases, partial melts of the lower crust and/or slab will interact with peridotitic mantle during their ascent, resulting in characteristically high MgO, Cr and Ni contents (Rapp et al., 1999; Smithies, 2000; Prouteau et al., 2001; Martin et al., 2005; Wang et al., 2006a) (Fig. 10). In addition, most modern slab-derived adakites have MORB-like Sr–Nd–Hf isotopic compositions and OIB-like trace element distributions (e.g., Stern and Kilian, 1996; Sajona et al., 2000). These predicted characteristics are not observed in the Mopanshan samples. In

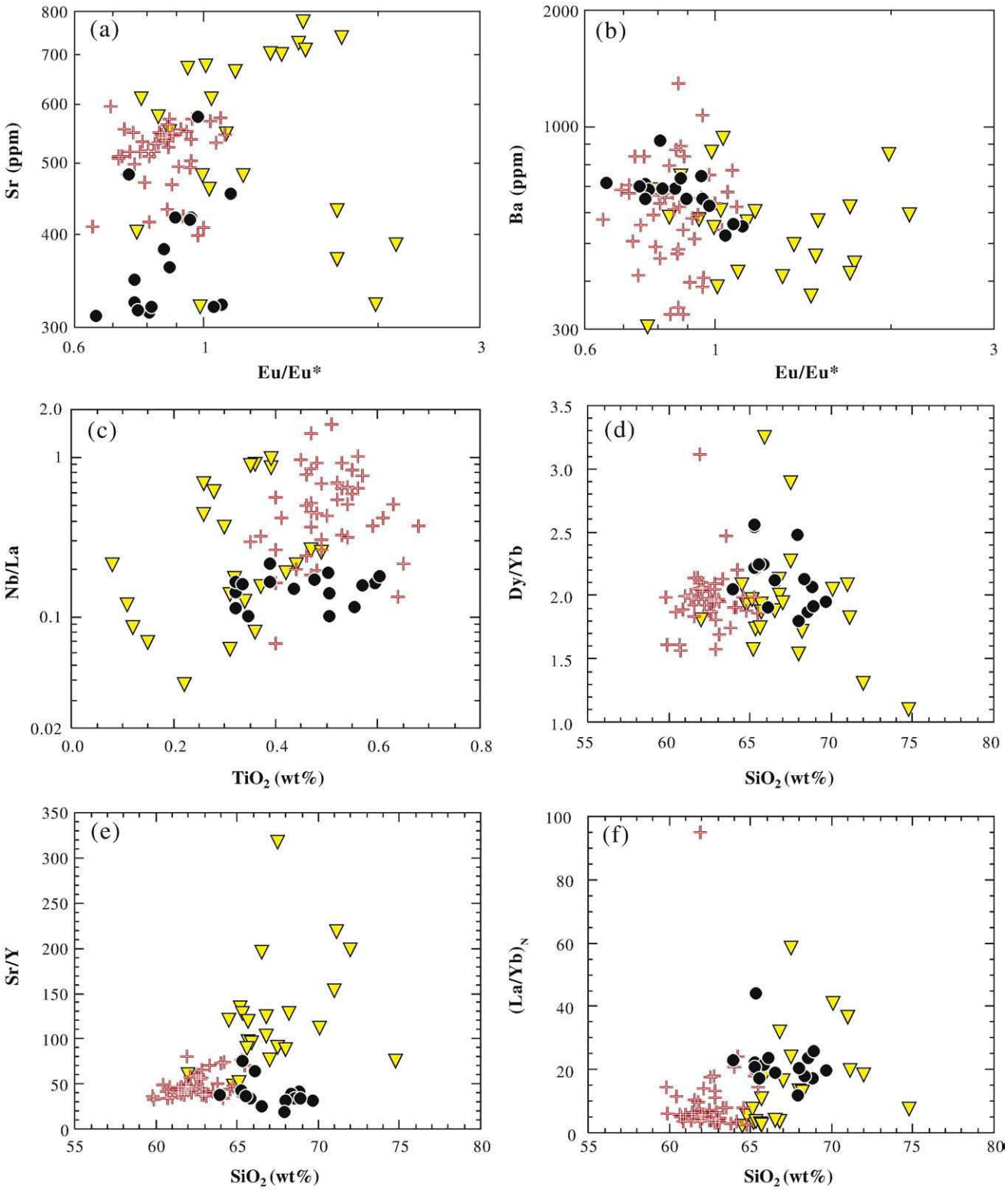

Fig. 8. Plots of Sr vs Eu/Eu*, Ba vs Eu/Eu*, Nb/La vs TiO_2, Dy/Yb vs SiO_2, Sr/Y vs SiO_2 and $(La/Yb)_N$ vs SiO_2 for the Mopanshan adakitic rocks. Data sources and symbols as in Fig. 5.

contrast, the negative $\varepsilon_{Nd}(t)$ values and arc-like pattern of trace element distribution in the Mopanshan samples are very similar to the thickened lower crust-derived adakites, which is also compatible with the features of low MgO (0.88–2.14 wt.%), Cr and Ni (5.21–31.1 ppm and 1.64–11.6 ppm, respectively; Table 3), and high SiO_2 (63.92–69.69 wt.%) contents (Fig. 10). Although the terrigeneous sediments in subduction zones might contribute to the negative $\varepsilon_{Nd}(t)$ values and arc-like pattern of the trace element distribution, the presence of terrigeneous sediments does not explain the presence of inherited zircons or the low MgO, Cr, Ni and high SiO_2 contents of the Mopanshan samples.

Zircon Hf isotopes place further constraints on the nature of the crustal source of the Mopanshan adakites. Geochemical differentiation produces a continental crust with Lu/Hf ratios significantly lower than the upper mantle, making initial $^{176}Hf/^{177}Hf$ ratios

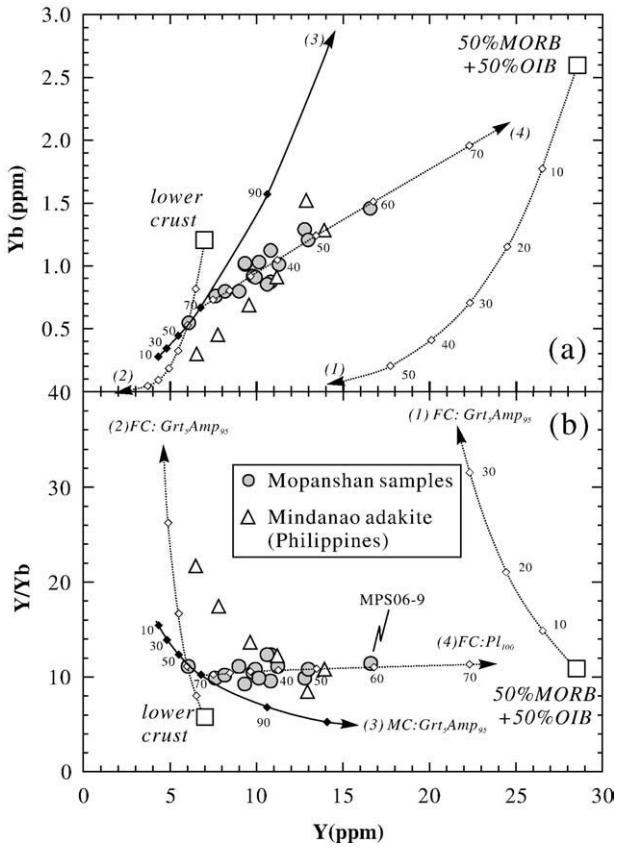

Fig. 9. Plots of Yb and Y/Yb vs. Y for the Mopanshan adakitic rocks. Fractional melting curve (MC) and Rayleigh fractionation curves (FC) were calculated for (1) FC for basalt crystallizing 5% garnet and 95% amphibole; (2) FC for lower crust crystallizing 5% garnet and 95% amphibole; (3) MC for lower crust leaving residues of 5% garnet and 95% amphibole (garnet amphibolite); (4) Melts generated by 70% partial melting of the lower crust, followed by plagioclase fractionation. Partition coefficients for andesitic melts (GERM website) were used in the calculation: amphibole (Yb = 2.1, Y = 1.47), garnet (Yb = 53, Y = 5.8), plagioclase (Yb = 0.1, Y = 0.01). Data sources: lower crust (Weaver and Tarney, 1984), OIB and N-MORB (Sun and McDonough, 1989), Mindanao adakites (Macpherson et al., 2006).

unambiguous petrogenetic indicators of crustal or mantle derivation (Zheng et al., 2006).

The positive $\varepsilon_{Hf}(t)$ values (1.91–7.07; Table 2) in zircons from Mopanshan indicate the involvement of mantle-derived components in their petrogenesis. These $\varepsilon_{Hf}(t)$ values are distinctively lower than those of the depleted mantle (Fig. 11a), suggesting crustal contamination during magma emplacement or derivation from a reworked crust. The involvement of old crustal materials is also evident given the presence of inherited zircons in the Mopanshan samples.

The zircon $\varepsilon_{Hf}(t)$ values (4.23 to 7.07, Table 2) of the Mopanshan adakitic rocks deviate from the whole-rock negative $\varepsilon_{Nd}(t)$ values (−2.06 to −0.43; Table 4) of the average arrays of mantle and crust Hf–Nd isotope evolution (Vervoort et al., 1999) (Fig. 11b), suggesting some Hf–Nd isotope decoupling. Because some relict zircons show relatively low $\varepsilon_{Hf}(t)$ values (calculated for 780 Ma) close to the Hf–Nd terrestrial array (Fig. 11b; Table 2), it is suggested that the decoupling of zircon Hf isotopes from the whole-rock Nd isotopes of the Mopanshan adakitic rocks was likely due to retention of radiogenic Hf in igneous zircons during partial melting of ancient crust (Zheng et al., 2007) or the contamination of ancient crust during magma evolution. We thus suggest that the source of the Mopanshan adakitic rocks may be reworked crust.

Experimental studies have suggested that melting of mafic materials produces adakitic magmas at pressures greater than 1.2 GPa, with a residual phase containing garnet but no plagioclase (Rapp and Watson, 1995; Rapp et al., 1999). The depletion in Y and HREE in the Mopanshan adakitic rocks implies significant amounts of residual garnet ± amphibole in the source. Whether the residual mineral is garnet or amphibole will lead to different trace element signatures. If garnet is residual in the source, the resultant magmas show not only a strong HREE depletion, but also a progressive decrease in HREE with increasing atomic number according to the partition coefficients for these elements (Rollinson, 1993, and references therein). If amphibole is residual in the source it will induce concave-upward

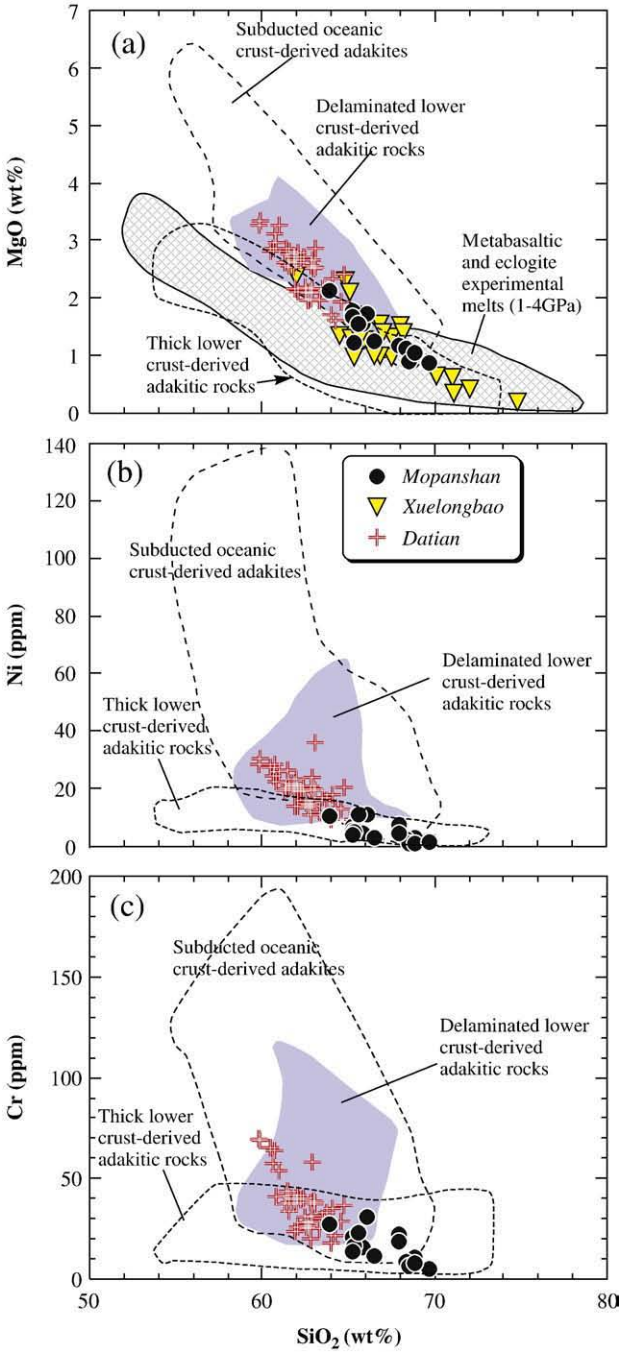

Fig. 10. Plots of MgO, Ni and Ni vs. SiO_2 for the Mopanshan adakitic rocks. Fields of subducted oceanic crust- and delaminated lower crust-derived adakites and metabasaltic and eclogite experimental melts are after the compilations of Wang et al. (2006a). Field of thick lower crust-derived adakitic rocks are from the following: Atherton and Petford (1993), Muir et al. (1995), Petford and Atherton (1996), Johnson et al. (1997), Xiong et al. (2003) and Wang et al. (2006b). Data sources: Xueolongbao (Zhou et al., 2006a), Datian (Zhao and Zhou, 2007).

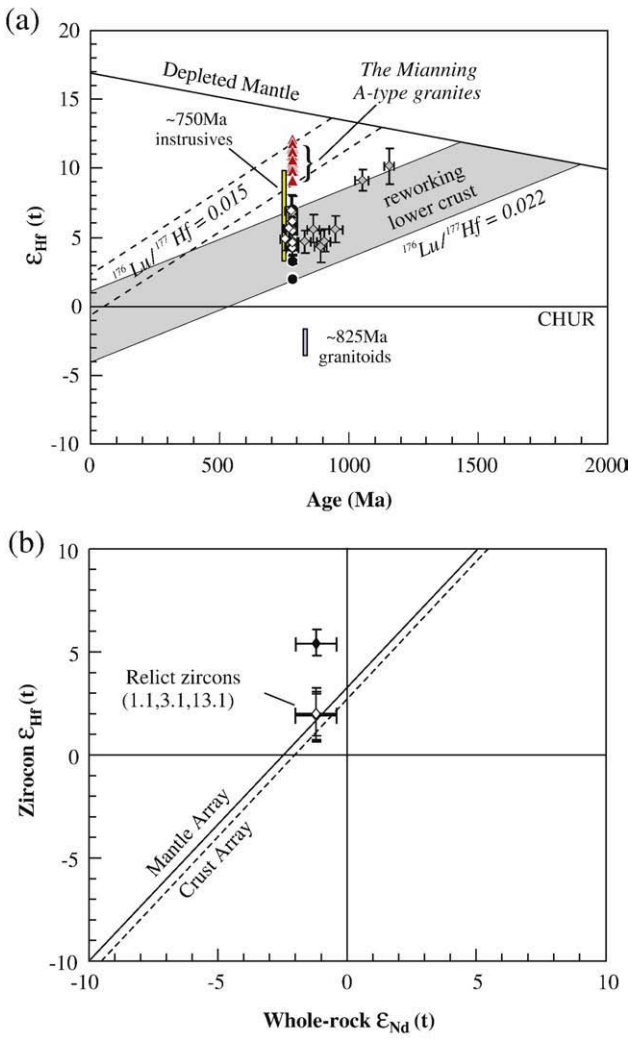

Fig. 11. (a) Diagram of Hf isotope evolution in the zircon from the Mopanshan adakitic rocks; The evolution of depleted mantle (DM) is drawn by using a present-day $^{176}Hf/^{177}Hf = 0.28325$ and $^{176}Lu/^{177}Hf = 0.0384$ (Griffin et al., 2000). The corresponding lines of crustal extraction are calculated by assuming the $^{176}Lu/^{177}Hf$ ratio of 0.015 for the averaged continental crust in the Mianning A-type granite and $^{176}Lu/^{177}Hf$ ratio of 0.022 for the lower crust (Amelin et al., 2000) in the Mopanshan adakitic rocks. (b) Relationship between zircon Hf and whole-rock Nd isotopes for the Mopanshan adakitic rocks. Mantle array and crust array are from Vervoort et al. (1999).

patterns between middle and heavy REE because of its high partition coefficients for these elements in intermediate to felsic melts (Rollinson, 1993, and references therein). The relatively flat HREE patterns (Fig. 5a) of the Mopanshan adakitic rocks are thus indicative of dominant amphibole with minor garnet in the residue (Figs. 6a and 9). On the other hand, the presence of residual rutile in the source will cause the depletions of both Nb–Ta and Ti in the partial melting products of subducted oceanic crust (Pearce and Norry, 1979; Xiong et al., 2005). However, rutile as a residual phase is not required because the Nb–Ta–Ti depletion could be inherited from previous histories of source materials. The strong depletions of both Nb–Ta and Ti in the Mopanshan samples (Fig. 5b) are likely features of the crustal source which formed during the orogenic events of 1.0–0.9 Ga in western South China (Li et al., 1995).

5.2. Petrogenetic evaluation of Neoproterozoic adakites from the western Yangtze Craton and tectonic implications

Igneous rocks form the Latest Mesoproterozoic to middle Neoproterozoic (ca. 1050–740 Ma) are widespread along the western margin of the Yangtze Block (Li et al., 2006a). Although it is commonly suggested that the orogenic events in western South China took place at 1.0–0.9 Ga (Li et al., 1995), the tectonic regime of the Neoproterozoic magmatism (860–740 Ma) in south China remains controversial. One opinion is that this magmatism was generated in an anorogenic setting, and that the region was under extension at 860–750 Ma and became part of a failed continental rift (the Kangdian Rift) during the 830–740 Ma interval (e.g., Li et al., 2002a, 2003, 2006a). An alternate model of plate-rift suggests that ~780 and ~825 Ma magmatism corresponds respectively to syn-rift and pre-rift magmatic events in response to super-continental rifting (Zheng et al., 2007, 2008), and indicates reworking of late Mesoproterozoic juvenile crust for the origin of the Neoproterozoic magmatic rocks or rifting anatexis of ancient Middle Paleoproterozoic crust (Zheng et al., 2008, 2009). However, the competing model suggests that the orogenic events in western South China lasted until ~750 Ma (Zhou et al., 2002, 2006a,b). Petrogenetic interpretation of Neoproterozoic adakites plays a critical role in formulating the arc model. For instance, Zhou et al. (2006a) interpreted the Xuelongbao adakitic complex to be the result of partial melting of subducted oceanic slab, in support of an arc setting during the Neoproterozoic time in south China. Our data collected on the Mopanshan adakites offer new interpretations for the Neoproterozoic tectonic setting in South China. As demonstrated in the previous section, the source of the Mopanshan adakites is interpreted as a reworked lower crust rather than a subducted oceanic slab. This implies an intraplate environment during the Neoproterozoic in South China, consistent with the rift setting as inferred from the contemporaneous Mianning A-type granites (Huang et al., 2008), Suxiong bimodal volcanism (Li et al., 2002a) and juvenile crustal components identified in the ~750 Ma granitoids (Zheng et al., 2007). Clearly, the proponents of different models heavily rely on the petrogenetic interpretation of the Neoproterozoic adakites from the western Yangtze craton.

Adakitic intrusions from Xuelongbao (750 Ma) and Datian (760 Ma) (Fig. 1) are located in the western Yangtze craton and have been interpreted as partial melts of subducted oceanic slabs (Zhou et al., 2006a; Zhao and Zhou, 2007). These adakitic suites are compared with the Mopanshan samples in Figs. 4–6, 8 and 10. It is clear that the Mopanshan adakitic rocks and the Xuelongbao adakitic complex show similar major and trace element compositions, with the latter having slightly higher K_2O and Yb contents and lower Sr/Y ratios (Figs. 4 and 6). The Datian adakitic intrusions display lower SiO_2 and higher MgO, Cr and Ni contents than the Mopanshan and Xuelongbao adakites (Zhao and Zhou, 2007). In their petrogenetic discussions (Zhou et al., 2006a; Zhao and Zhou, 2007), the low contents of K, Th and low K_2O/Na_2O ratios (high Na_2O contents) have been considered important evidence for slab melting, in contrast with the high-K contents in continental lower crust-derived adakites (Fig. 12). A relevant question is whether the high K content in adakites is diagnostic of a continental crust origin.

In seeking an answer to this question, we have compiled data available for adakites, which are categorized as two groups in terms of petrogenetic interpretation: slab-derived and lower crust-derived (see Fig. 12). Unlike Zhou et al. (2006a) and Zhao and Zhou (2007) who only used the Tibetan adakites as the example of continental crust-derived adakites, our compilation includes data for worldwide adakites (Atherton and Petford, 1993; Muir et al., 1995; Petford and Atherton, 1996; Johnson et al., 1997; Xu et al., 2002; Xiong et al., 2003; Wang et al., 2004a,b, 2006a,b). It is clear from Fig. 12 that, if the Tibetan adakites are excluded, the slab-derived and thickened crust-derived adakites largely overlap in plots involving K_2O, Na_2O and Th/La and Th/Nb ratios. For instance, typical thickened lower crust-derived adakitic rocks reported by Atherton and Petford (1993) and Petford and Atherton (1996) are characterized by low K_2O contents, low Th/La and Th/Nb ratios and high Na_2O contents, indistinguishable from those derived from oceanic slabs. In our opinion, the low K, Th and high Na_2O contents cannot be taken as diagnostic indicators for slab-derived

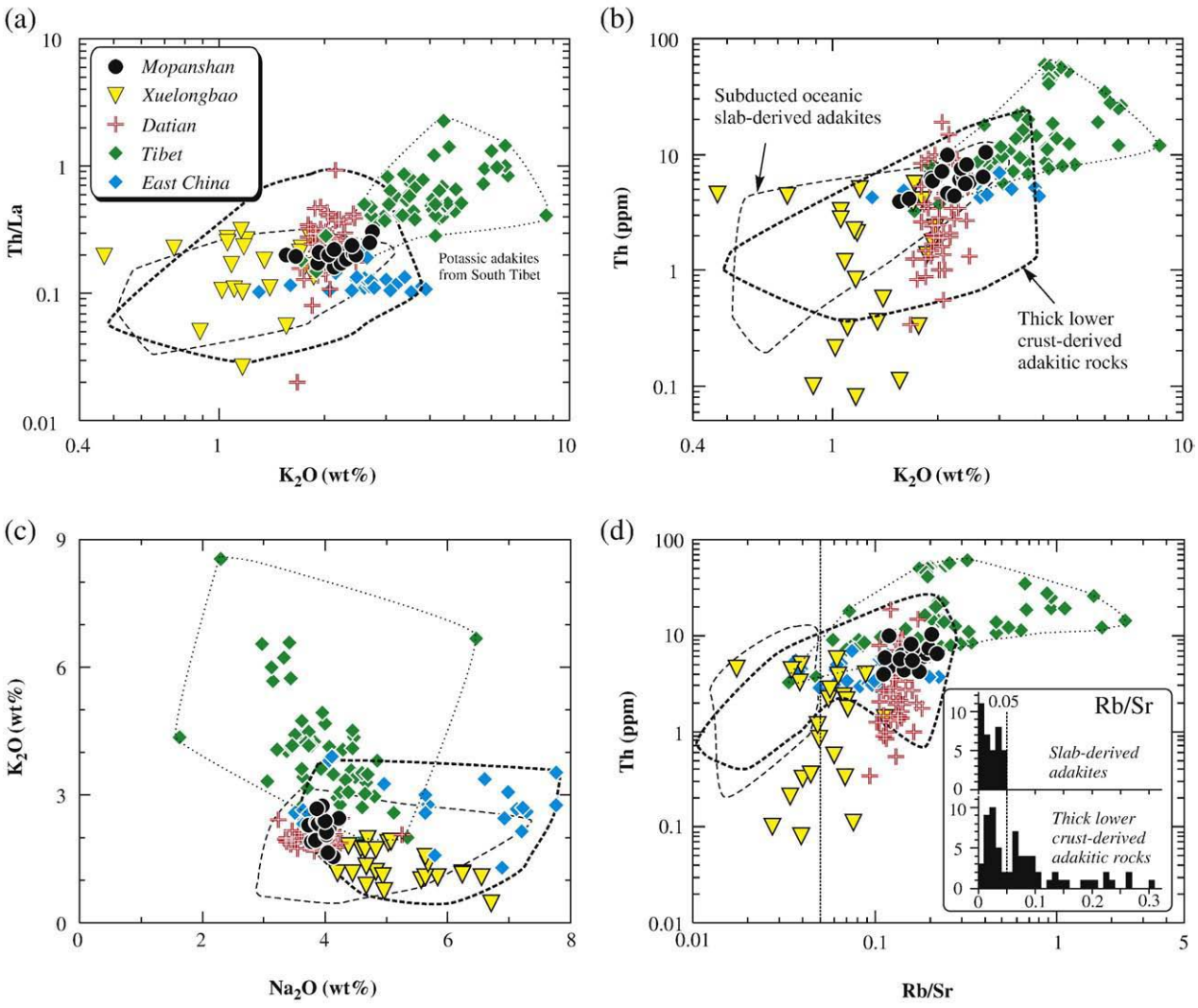

Fig. 12. Plots of (a) Th/La vs. K_2O; (b) Th vs. K_2O; (c) K_2O vs Na_2O; and (d) Th/Nb vs. Rb/Sr for the Mopanshan adakitic rocks. Data sources: Xueolongbao (Zhou et al., 2006a), Datian (Zhao and Zhou, 2007), Tibet (Chung et al., 2003; Wang et al., 2005), East China (Xiong et al., 2003; Wang et al., 2006b). The inset histogram in (d) shows that typical slab-derived adakites (Data sources: Defant and Drummond, 1990; Kay et al., 1993; Drummond et al., 1996; Stern and Kilian, 1996; Sajona et al., 2000; Aguillón-Robles et al., 2001; Martin et al., 2005) generally have low Rb/Sr ratios (<0.05), and that typical thick lower crust-derived adakites (Data sources: Atherton and Petford, 1993; Muir et al., 1995; Petford and Atherton, 1996; Johnson et al., 1997) have wide range of Rb/Sr ratios.

adakites. Our compilation also highlights the compositional particularity of the Tibetan adakites with anomalously high K_2O content and Th/La ratios (Fig. 12), which had been explained by additional input of ultra-potassic magmas during formation or migration of pristine adakitic melts (Hou et al., 2004; Guo et al., 2007). Given the considerable debate on the origin of the Tibetan adakites (Chung et al., 2003; Hou et al., 2004; Guo et al., 2007) and the reasons mentioned above, it is inappropriate to take the Tibetan adakites as representative of continental crust-derived adakites.

More importantly, unlike most modern slab-derived adakites that have MORB-like Nd isotopic compositions (e.g., Stern and Kilian, 1996; Sajona et al., 2000), both the Xuelongbao and Datian adakitic rocks display low $\varepsilon_{Nd}(t)$ values (0.36–2.88 and −0.92 to 0.62; respectively; Zhou et al., 2006a; Zhao and Zhou, 2007), significantly lower than those of Neoproterozoic basaltic rocks in the western Yangtze craton (Fig. 7b) (Li et al., 2007a). In addition, available data for adakites worldwide indicate that typical slab melts generally have low Rb/Sr ratios (0.01–0.05; Fig. 12d), in contrast to the wide range of Rb/Sr ratios (0.01–0.4) for the adakites derived from thickened crust (Fig. 12d). The majority of Neoproterozoic adakites from western Yangtze Craton have high Rb/Sr ratios (Fig. 12d), thereby arguing against slab melting and indicating a large contribution of the lower crust in their generation. Hence, both elemental and isotopic compositions of the Neoproterozoic adakitic rocks from the western Yangtze Craton are consistent with the model involving partial melting of thickened mafic lower crust. Different Sr/Y ratios and Yb contents between Xuelongbao and Mopanshan adakitic rocks may be attributed to different residual components in the sources (Fig. 6a). The elevated MgO, Cr and Ni contents of the Datian adakitic rocks may be related to a higher degree of partial melting of the mafic lower crust as indicated by the low $(La/Yb)_N$ ratios and SiO_2 contents (Figs. 6a; 8f).

The above petrogenetic re-evaluation leads to the suggestion that the Neoproterozoic adakites from the western margin of the Yangtze Craton were formed by partial melting of a thickened lower crust in an intraplate setting. This is consistent with the occurrence of contemporaneous Mianning A-type granites (~780 Ma; Huang et al., 2008), the Suxiong bimodal volcanic rocks (803 ± 12 Ma; Li et al., 2002a) and other 780–750 Ma bimodal intrusives in the rifted tectonic zone (Zheng et al., 2006, 2007; Chen et al., 2007; Zhao et al., 2008), which are products of rift magmatism in response to Rodinia breakup and indicative of an anorogenic, crustal extensional environment for the western Yangtze Craton during the Neoproterozoic.

The thickening of continental lithosphere generally takes place along the margin of convergent plates such as in collision orogens. The Rodinia supercontinent was assembled through worldwide Grenville-aged (1300 Ma–900 Ma) orogenic events (e.g., Hoffman, 1991; Li et al., 2008). The Yangtze block may have been a continental fragment caught between Australia and Laurentia during the assembly of Rodinia (Li et al., 1995, 2008), or located on the periphery of Rodinia during the early Neoproterozoic (Zhou et al., 2006a). In any case, the western Yangtze Craton was in a convergent tectonic setting at that time, and the Sibao Orogeny in South China is one of the Grenville-aged orogenic belts (Li et al., 2002b, 2006a, 2007b). The old inherited zircons in MPS05-3 have $^{206}Pb/^{238}U$ age of 1.05–1.16 Ga, contemporaneous with the peak of the Sibao Orogeny (e.g., Li et al., 2002b; Greentree et al., 2006; Li et al., 2007b). We thus suggest that the crust was thickened during the Sibao Orogeny. Zheng et al. (2007, 2008, 2009) have addressed the same issue in detail within the framework of the plate-rift model. The attributes of orogenic lithosphere are susceptible to reactivation by extensional tectonics and thermal anomalies. Ancient collisional belts in the western Yangtze Craton are favorite places for orogenic collapse, rift magmatism and continental breakup (Zheng et al., 2007, 2008, 2009). The old tectonic belts not only affect the location of rifting, but also the inherited lithosphere architecture plays a role in the rifting process itself, the thermal evolution of the rift, and decompression melting of asthenospheric mantle and thus growth of juvenile crust during rifting (Zheng et al., 2008, 2009). Thus, it is possible that the Rodinia breakup would be initiated in the Grenvillian arc-continent collision belts, and was contemporaneous with emplacement of large igneous provinces at about 780 to 740 Ma in South China (Zheng et al., 2009). Thus, the Mopanshan adakitic rocks were likely generated by partial melting of a thickened lower crust triggered by crustal extension. However, the data presented in this study are not sufficient to identify the ultimate mechanism for the Neoproterozoic tectonic framework of South China or if a plume was involved in the Neoproterozoic magmatism.

5.3. Implications for crustal evolution in south China

While zircon U–Pb ages register magmatic episodes related to crustal reworking or crustal growth with juvenile material addition, zircon Hf model ages provide a first approximation to timing of crustal extraction from the mantle when its initial Hf isotope composition approaches that of the contemporaneous depleted mantle (e.g., Griffin et al., 2000; Hawkesworth and Kemp, 2006; Zheng et al., 2006). The Mopanshan zircon Hf model ages (1064–1276 Ma; Table 2) are younger than the whole-rock Nd model ages (1281–1464 Ma; Table 4). This difference may be related to the modification of Nd isotopes during crustal reworking and the preservation of initial $\varepsilon_{Hf}(t)$ values owing to the resistance of zircon during most geological processes. This is also reflected by the Hf–Nd decoupling as illustrated in Fig. 11. Therefore, the Mopanshan zircon Hf model ages (1064–1276 Ma; Table 2) provide a reasonable proxy for timing of juvenile crust growth (Nebel et al., 2007; Zheng et al., 2007), suggesting the late Mesoproterozoic growth of juvenile crust in western South China, during the Sibao orogenic events (Li et al., 2006a; Greentree et al., 2006; Zheng et al., 2007). The late Mesoproterozoic growth of juvenile crust occurred not only in western South China, but also in northern South China (Chen et al., 2007; Zheng et al., 2008, 2009) and southeastern South China (Wu et al., 2006a,b; Zheng et al., 2008). In addition, Hf model ages for the Mopanshan inherited zircons are about 0.1–0.4 Ga older (Table 2) than their $^{206}Pb/^{238}U$ ages, suggesting that they have crystallized from a source which incorporated certain amounts of old crustal components. The U–Pb ages of inherited zircons (829–1051 Ma; Table 2) in the Mopanshan adakitic rocks recorded episodic crustal growth and reworking since the Sibao Orogeny, an inference supported by the widespread igneous rocks from latest Mesoproterozoic to middle Neoproterozoic along the western margin of the Yangtze Block (Li et al., 2002a,b, 2006a).

6. Conclusions

On the basis of new geochronological, geochemical and Nd–Hf isotopic data, the following conclusions can be drawn regarding the origin and tectonic setting of the Mopanshan adakitic rocks:

(1) Zircon U–Pb dating indicates that the Mopanshan adakitic rocks in the north Kangdian rift were emplaced at ~780 Ma, contemporaneous with the widespread Neoproterozoic anorogenic magmatism in South China.
(2) The Mopanshan adakitic rocks were generated by partial melting of a juvenile, thickened lower crust in an intracontinental setting. A similar petrogenetic model can be applied to the Xuelongbao and Datian adakites of the western Yangtze Craton, which have previously been interpreted as slab-derived melts. Partial melting of a thickened lower crust underneath the western Yangtze Craton during the Neoproterozoic was likely triggered by crustal extension.
(3) Zircon Hf model ages (1064–1276 Ma) for the Mopanshan adakites provide evidence for and timing of the juvenile crust growth during the late Mesoproterozoic in the western Yangtze Craton. The incorporation of old crustal components in the source of the Mopanshan adakites reflects crustal reworking since the Sibao Orogeny.

Acknowledgements

We gratefully acknowledge the careful and constructive comments of Y.L. Niu, Y.F. Zheng, N. Eby and an anonymous reviewer, which considerably improved the manuscript. We appreciate Y. Liu, X.L. Tu, X.R. Liang, Y.B. Wang (Beijing SHRIMP Center) and H.H. Zhang for assistance in major element, trace element, Sr–Nd isotope analyses, zircon U–Pb dating and Lu–Hf isotope analyses, respectively. Dr. Q. Wang is thanked for helpful discussions. This work was supported by the National Science Foundation of China (NSFC grants 40721063), the Chinese Academy of Sciences (KZCX2-YW-Q08-3-6 and KZCX1-YW-15-2) and the CAS/SAFEA International Partnership Program for Creative Research Teams. This is contribution No. IS-1049 from GIGCAS.

References

Aguillón-Robles, A., Calmus, T., Bellon, H., Maury, R.C., Cotten, J., Bourgois, J., Michaud, F., 2001. Late Miocene adakites and Nb-enriched basalts from Vizcaino Peninsula, Mexico: indicators of East Pacific Rise subduction below southern Baja California. Geology 29, 531–534.
Amelin, Y., Lee, D.-C., Halliday, A.N., 2000. Early-middle archaean crustal evolution deduced from Lu-Hf and U-Pb isotopic studies of single zircons grains. Geochimica et Cosmochimica Acta 64, 4205–4225.
Atherton, M.P., Petford, N., 1993. Generation of sodium rich magmas from newly underplated basaltic crust. Nature 362, 144–146.
Blichert-Toft, J., Albarede, F., 1997. The Lu–Hf geochemistry of chondrites and the evolution of the mantle–crust system. Earth and Planetary Science Letters 148, 243–258.
Castillo, P.R., 2006. An overview of adakite petrogenesis. Chinese Science Bulletin 51, 257–268.
Castillo, P.R., Janney, P.E., Solidum, R.U., 1999. Petrology and geochemistry of Camiguin island, southern Philippines: insights to the source of adakites and other lavas in a complex arc setting. Contributions to Mineralogy and Petrology 134, 33–51.
Chen, R.X., Zheng, Y.F., Zhao, Z.F., Tang, J., Wu, F.Y., Liu, X.M., 2007. Zircon U–Pb ages and Hf isotopes in ultrahigh-pressure metamorphic rocks from the Chinese Continental Scientific Drilling project. Journal of Metamorphic Geology 25, 873–894.
Chung, S.L., Liu, D.Y., Ji, J.Q., Chu, M.F., Lee, H.Y., Wen, D.J., Lo, C.H., Lee, T.Y., Qian, Q., Zhang, Q., 2003. Adakites from continental collision zones. Melting of thickened lower crust beneath southern Tibet. Geology 31, 1021–1024.
Condie, K.C., 2005. TTGs and adakites: are they both slab melts? Lithos 80, 33–44.
Defant, M.J., Drummond, M.S., 1990. Derivation of some modern arc magmas by melting of young subducted lithosphere. Nature 347, 662–665.
DePaolo, D.J., 1981. A neodymium and strontium isotopic study of the Mesozoic calc-alkaline granitic batholiths of the Sierra Nevada and Peninsular Ranges, California. Journal of Geophysical Research 86, 10470–10488.
Drummond, M.S., Defant, M.J., 1990. A model for trondhjemite–tonalite–dacite genesis and crustal growth via slab melting: Archean to modern comparisons. Journal of Geophysical Research 95, 21503–21521.

Drummond, M.S., Defant, M.J., Kepezhinskas, P.K., 1996. Petrogenesis of slab-derived trondhjemite–tonalite–dacite/adakite magmas. Transactions of the Royal Society of Edinburgh. Earth Sciences 87, 205–215.
GERM (Geochemical Earth Reference Model) home page. http://www.earthref.org.
Greentree, M.R., Li, Z.X., Li, X.H., Wu, H., 2006. Late Mesoproterozoic to earliest Neoproterozoic basin record of the Sibao orogenesis in western South China and relationship to the assembly of Rodinia. Precambrian Research 151, 79–100.
Griffin, W.L., Pearson, N.J., Belousova, E., Jackson, S.E., O'Reilly, S.Y., van Achterberg, E., Shee, S.R., 2000. The Hf isotope composition of cratonic mantle: LAM-MC-ICPMS analysis of zircon megacrysts in kimberlites. Geochimica et Cosmochimica Acta 64, 133–147.
Griffin, W.L., Pearson, N.J., Belousova, E.A., Saeed, A., 2006. Comment: Hf-siotope heterogeneity in zircon 91500. Chemical Geology 233, 358–363.
Guo, Z.F., Wilson, M., Liu, J.Q., 2007. Post-collisional adakites in south Tibet: products of partial melting of subduction-modified lower crust. Lithos 96, 205–224.
Hawkesworth, C.J., Kemp, A.I.S., 2006. Using hafnium and oxygen isotopes in zircons to unravel the record of crustal evolution. Chemical Geology 226, 144–162.
He, J., Chen, G., Yang, T., Min, J., 1988. The Kandian Grey Gneisses. Chongqing Publishing House, Chongqing. (in Chinese).
Hoffman, P.F., 1991. Did the breakout of Laurentia turn Gondwanaland inside-out? Science 252, 1409–1412.
Hou, Z.Q., Gao, Y.F., Qu, X.M., Rui, Z.Y., Mo, X.X., 2004. Origin of adakitic intrusives generated during mid-Miocene east-west extension in southern Tibet. Earth and Planetary Science Letters 220, 139–155.
Huang, X.L., Xu, Y.G., Li, X.H., Li, W.X., Lan, J.B., Zhang, H.H., Liu, Y.S., Wang, Y.B., Li, H.Y., Luo, Z.Y., Yang, Q.J., 2008. Petrogenesis and tectonic implications of Neoproterozoic, highly fractionated A-type granites from Mianning, South China. Precambrian Research 165, 190–204.
Johnson, K., Barnes, C.G., Miller, C.A., 1997. Petrology, geochemistry, and genesis of high-Al tonalite and trondhjemites of the Cornucopia stock, Blue Mountains, Northeastern Oregon. Journal of Petrology 38, 1585–1611.
Kay, S.M., Ramos, V.A., Marquez, M., 1993. Evidence in Cerro Pampa volcanic rocks for slab-melting prior to ridge-trench collision in southern South America. Journal of Geology 101, 703–714.
Li, X.H., 1997. Geochemistry of the Longsheng Ophiolite from the southern margin of Yangtze Craton, SE China. Geochemical Journal 31, 323–337.
Li, Z.X., Zhang, L., Powell, C.M., 1995. South China in Rodinia: part of the missing link between Australia–East Antarctica and Laurentia? Geology 23, 407–410.
Li, Z.X., Li, X.H., Kinny, P.D., Wang, J., 1999. The breakup of Rodinia: did it start with a mantle plume beneath South China? Earth and Planetary Science Letters 173, 171–181.
Li, X.H., Li, Z.X., Zhou, H.W., Liu, Y., Kinny, P.D., 2002a. U–Pb zircon geochronology, geochemistry and Nd isotopic study of Neoproterozoic bimodal volcanic rocks in the Kangdian Rift of South China: implications for the initial rifting of Rodinia. Precambrian Research 113, 135–154.
Li, Z.X., Li, X.H., Zhou, H., Kinny, P.D., 2002b. Grenvillian continental collision in South China: new SHRIMP U–Pb zircon results and implications for the configuration of Rodinia. Geology 30, 163–166.
Li, X.H., Li, Z.X., Zhou, H.W., Liu, Y., Liang, X.R., 2002c. U–Pb zirocn geochronological, geochemical and Nd isotopic study of Neoproterozoic basaltic magmatism in Western Sichuan: petrogenesis and geodynamic implications. Earth Science Frontiers 9 (4), 329–338 (in Chinese with English abstract).
Li, Z.X., Li, X.H., Kinny, P.D., Wang, J., Zhang, S., Zhou, H., 2003. Geochronology of Neoproterozoic syn-rift magmatism in the Yangtze Craton, South China and correlations with other continents: evidence for a mantle superplume that broke up Rodinia. Precambrian Research 122, 85–109.
Li, X.H., Li, Z.X., Ge, W.C., Zhou, H.W., Li, W.X., Liu, Y., Wingate, M.T.D., 2004a. Reply to the comment: mantle plume-,but not arc-related Neoproterozoic magmatism in South China. Precambrian Research 132, 405–407.
Li, X.H., Liu, D.Y., Sun, M., Li, W.X., Liang, X.R., Liu, Y., 2004b. Precise Sm–Nd and U–Pb isotopic dating of the super-giant Shizhuyuan polymetallic deposit and its host granite, Southeast China. Geological Magazine 141, 225–231.
Li, X.H., Li, Z.X., Sinclair, J.A., Li, W.X., Carter, G., 2006a. Revisiting the "Yanbian Terrane": implications for Neoproterozoic tectonic evolution of the western Yangtze Block, South China. Precambrian Research 151, 14–30.
Li, X.H., Li, Z.X., Wingate, M.T.D., Chung, S.L., Liu, Y., Lin, G.C., Li, W.X., 2006b. Geochemistry of the 755 Ma Mundine Well dyke swarm, northwestern Australia: part of a Neoproterozoic mantle superplume beneath Rodinia? Precambrian Research 146, 1–15.
Li, X.H., Li, Z.X., Sinclair, J.A., Li, W.X., Carter, G., 2007a. Reply to the comment by Zhou et al. on: "Revisiting the "Yanbian Terrane": implications for Neoproterozoic tectonic evolution of the western Yangtze Block, South China" [Precambrian Res. 151 (2006) 14–30] [Precambrian Res. 154 (2007) 153–157]. Precambrian Research 155, 318–323.
Li, Z.X., Wartho, J.A., Occhipinti, S., Zhang, C.L., Li, X.H., Wang, J., Bao, C., 2007b. Early history of the eastern Sibao Orogen (South China) during the assembly of Rodinia: new mica $^{40}Ar/^{39}Ar$ dating and SHRIMP U–Pb detrital zircon provenance constraints. Precambrian Research 159, 79–94.
Li, Z.X., Bogdanova, S.V., Collins, A.S., Davidson, A., De Waele, B., Ernst, R.E., Fitzsimons, I.C.W., Fuck, R.A., Gladkochub, D.P., Jacobs, J., Karlstrom, K.E., Lu, S., Natapov, L.M., Pease, V., Pisarevsky, S.A., Thrane, K., Vernikovsky, V., 2008. Assembly, configuration, and break-up history of Rodinia: a synthesis. Precambrian Research 160, 179–210.
Lin, G.C., Li, X.H., Li, W.X., 2007. SHRIMP U–Pb zircon age, geochemistry and Nd–Hf isotopes of the Neoproterozoic mafic dykes from western Sichuan: petrogenesis and tectonic implications. Science in China. Series D 50, 1–16.
Liu, H., 1991. Classification of Sinian system. In: Liu, H. (Ed.), The Sinian System in China. Science Press, Beijing, pp. 115–125 (in Chinese).
Macpherson, C.G., Dreher, S., Thirlwall, M.F., 2006. Adakites without slab melting: high pressure differentiation of island arc magma, Mindanao, the Philippines. Earth and Planetary Science Letters 243, 581–593.
Martin, H., Smithies, R.H., Rapp, R., Moyen, J.F., Champion, D., 2005. An overview of adakite, tonalite–trondhjemite–granodiorite (TTG), and sanukitoid: relationships and some implications for crustal evolution. Lithos 79, 1–24.
Muir, R.J., Weaver, S.D., Bradshaw, J.D., Eby, G.N., Evans, J.A., 1995. Geochemistry of the Cretaceous Separation Point Batholith, New Zealand: granitoid magmas formed by melting of mafic lithosphere. Journal of the Geological Society London 152, 689–701.
Munteanu, M., Yao, Y., 2007. The Gaojiacun intrusion: rift- or subduction-related? A discussion on "Revisiting the "Yanbian Terrane": implications for Neoproterozoic tectonic evolution of the western Yangtze Block, South China" by Li et al. (2006). Precambrian Research 155, 164–167.
Nebel, O., Nebel-Jacobsen, Y., Mezger, K., Berndt, J., 2007. Initial Hf isotope compositions in magmatic zircon from early Proterozoic rocks from the Gawler Craton, Australia: a test for zircon model ages. Chemical Geology 241, 23–37.
Pearce, J.A., Norry, M.J., 1979. Petrogenetic implications of Ti, Zr, Y, and Nb variations in volcanic rocks. Contributions to Mineralogy and Petrology 69, 33–47.
Petford, N., Atherton, M., 1996. Na-rich partial melts from newly underplated basaltic crust: the Cordillera Blanca Batholith, Peru. Journal of Petrology 37, 1491–1521.
Prouteau, G., Scaillet, B., Pichavant, M., Maury, R.C., 2001. Evidence for mantle metasomatism by hydrous silicic melts derived from subducted oceanic crust. Nature 410, 197–200.
Rapp, R.P., Watson, E.B., 1995. Dehydration melting of metabasalt at 8–32 kbar: implications for continental growth and crust–mantle recycling. Journal of Petrology 36, 891–931.
Rapp, R.P., Shimizu, N., Norman, M.D., Applegate, G.S., 1999. Reaction between slab-derived melts and peridotite in the mantle wedge: experimental constraints at 3.8 GPa. Chemical Geology 160, 335–356.
Rollinson, H.R., 1993. Using geochemical data: evaluation, presentation, interpretation. Longman Singapore Publishers (Pte) Ltd., Singapore, pp. 1–352.
Sajona, F.G., Maury, R.C., Pubellier, M., Leterrier, J., Bellon, H., Cotten, J., 2000. Magmatic source enrichment by slab-derived melts in a young post-collision setting, central Mindanao (Philippines). Lithos 54, 173–206.
SBGMR (Sichuan Bureau of Geology and Mineral Resources), 1991. Regional Geology of Sichuan Province. Geological Publishing House, Beijing. (in Chinese with English abstract).
Smithies, R.H., 2000. The Archean tonalite–trondhjemite–granodiorite (TTG) series is not an analogue of Cenozoic adakite. Earth and Planetary Science Letters 182, 115–125.
Stern, C.R., Kilian, R., 1996. Role of the subducted slab, mantle wedge and continental crust in the generation of adakites from the Andean Austral Volcanic Zone. Contributions to Mineralogy and Petrology 123, 263–281.
Sun, S.-S., McDonough, W.F., 1989. Chemical and isotopic systematics of oceanic basalts: implications for mantle composition and processes. In: Saunders, A.D., Norry, M.J. (Eds.), Magmatism in the Ocean Basins. Geol. Soc. Spec. Publ., vol. 42, pp. 313–345.
Taylor, S.R., McLennan, S.M., 1985. The Continental Crust: Its Composition and Evolution. Blackwell, Oxford.
Vervoort, J.D., Patchett, P.J., Blichert-Toft, J., Albarede, F., 1999. Relationship between Lu–Hf and Sm–Nd isotopic systems in the global sedimentary system. Earth and Planetary Science Letters 168, 79–99.
Wang, Q., Zhao, Z.H., Bao, Z.W., Xu, J.F., Liu, W., Li, C.F., Bai, Z.H., Xiong, X.L., 2004a. Geochemistry and petrogenesis of the Tongshankou and Yinzu adakitic intrusive rocks and the associated porphyry copper–molybdenum mineralization in southeast Hubei, east China. Resource Geology 54, 137–152.
Wang, X., Zhou, J., Qiu, J., Gao, J., 2004b. Comment on "Neoproterozoic granitoids in South China: crustal melting above a mantle plume at ca. 825 Ma?" by Xian-Hua Li et al. (2003). Precambrian Research 132, 401–403.
Wang, Q., McDermott, F., Xu, J.F., Bellon, H., Zhu, Y.T., 2005. Cenozoic K-rich adakitic volcanics in the Hohxil area, northern Tibet: lower crustal melting in an intracontinental setting. Geology 33, 465–468.
Wang, Q., Xu, J.F., Jian, P., Bao, Z.W., Zhao, Z.H., Li, C.F., Xiong, X.L., Ma, J.L., 2006a. Petrogenesis of adakitic porphyries in an extensional tectonic setting, Dexing, South China: implications for the genesis of porphyry copper mineralization. Journal of Petrology 47, 119–144.
Wang, X.C., Liu, Y.S., Liu, X.M., 2006b. Mesozoic adakites in the Lingqiu Basin of the central North China Craton: partial melting of underplated basaltic lower crust. Geochemical Journal 40, 447–461.
Weaver, B.L., Tarney, J., 1984. Empirical approach to estimating the composition of the continental crust. Nature 310, 575–577.
Wei, G.J., Liang, X.R., Li, X.H., Liu, Y., 2002. Precise measurement of Sr isotopic compositions of liquid and solid base using (LP) MCICP-MS. Geochimica 31, 295–305 (in Chinese with English abstract).
Wiedenbeck, M., Hanchar, J.M., Peck, W.H., Sylvester, P., Valley, J., Whitehouse, M., Kronz, A., Morishita, Y., Nasdala, L., 2004. Further characterisation of the 91500 zircon crystal. Geostandards and Geoanalytical Research 28, 9–39.
Williams, I.S., 1998. U–Th–Pb geochronology by ion microprobe. In Applications of microanalytical techniques to understanding mineralizing processes. Review Economical Geology 7, 1–35.
Wu, F.Y., Yang, Y.H., Xie, L.W., Yang, J.H., Xu, P., 2006a. Hf isotopic compositions of the standard zircons and baddeleyites used in U–Pb geochronology. Chemical Geology 234, 105–126.
Wu, R.X., Zheng, Y.F., Wu, Y.B., Zhao, Z.F., Zhang, S.B., Liu, X.M., Wu, F.Y., 2006b. Reworking of juvenile crust: element and isotope evidence from Neoproterozoic granodiorite in South China. Precambrian Research 146, 179–212.

Xiong, X.L., Li, X.H., Xu, J.F., Li, W.X., Zhao, Z.H., Wang, Q., Chen, X.M., 2003. Extremely high-Na adakite-like magmas derived from alkali-rich basaltic underplate: the Late Cretaceous Zhantang andesites in the Huichang Basin, SE China. Geochemical Journal 37, 233–252.

Xiong, X.L., Adam, J., Green, T.H., 2005. Rutile stability and rutile/melt HFSE partitioning during partial melting of hydrous basalt: implications for TTG genesis. Chemical Geology 218, 339–359.

Xu, J.F., Shinjio, R., Defant, M.J., Wang, Q., Rapp, R.P., 2002. Origin of Mesozoic adakitic intrusive rocks in the Ningzhen area of east China: partial melting of delaminated lower continental crust? Geology 12, 1111–1114.

Xu, P., Wu, F., Xie, L., Yang, Y., 2004. Hf isotopic compositions of the standard zircons for U–Pb dating. Chinese Science Bulletin 49, 1642–1648.

Zhang, S.B., Zheng, Y.F., Zhao, Z.F., Wu, Y.B., Liu, X.M., Wu, F.Y., 2008. Neoproterozoic anatexis of Archean Lithosphere: geochemical evidence from felsic to mafic intrusives at Xiaofeng in the Yangtze George, South China. Precambrian Research 163, 210–238.

Zhao, J.H., Zhou, M.F., 2007. Neoproterozoic adakitic plutons and arc magmatism along the western margin of the Yangtze Block, South China. The Journal of Geology 115, 675–689.

Zhao, Z.F., Zheng, Y.F., Wei, C.S., Chen, F.K., Liu, X.M., Wu, F.Y., 2008. Zircon U–Pb ages, Hf and O isotopes constrain the crustal architecture of the ultrahigh-pressure Dabie orogen in China. Chemical Geology 253, 222–242.

Zheng, Y.F., Zhao, Z.F., Wu, Y.B., Zhang, S.B., Liu, X., Wu, F.Y., 2006. Zircon U–Pb age, Hf and O isotope constraints on protolith origin of ultrahigh-pressure eclogite and gneiss in the Dabie orogen. Chemical Geology 231, 135–158.

Zheng, Y.F., Wu, R.X., Wu, Y.B., Zhang, S.B., Yuan, H., Wu, F.Y., 2008. Rift melting of juvenile arc-derived crust: Geochemical evidence from Neoproterozoic volcanic and granitic rocks in the Jiangnan Orogen, South China. Precambrian Research 163, 351–383.

Zheng, Y.F., Zhang, S.B., Zhao, Z.F., Wu, Y.B., Li, X.H., Li, Z.X., Wu, F.Y., 2007. Contrasting zircon Hf and O isotopes in the two episodes of Neoproterozoic granitoids in South China: implications for growth and reworking of continental crust. Lithos 96, 127–150.

Zheng, Y.F., Chen, R.X., Zhao, Z.F., 2009. Chemical geodynamics of continental subduction-zone metamorphism: Insights from studies of the Chinese Continental Scientific Drilling (CCSD) core samples. Tectonophysics 464. doi:10.1016/j.tecto.2008.09.014.

Zhou, M.F., Yan, D.P., Kennedy, A.K., Li, Y., Ding, J., 2002. SHRIMP U–Pb zircon geochronological and geochemical evidence for Neoproterozoic arc-magmatism along the western margin of the Yangtze Block, South China. Earth and Planetary Science Letters 196, 51–67.

Zhou, M.F., Yan, D.P., Wang, C.L., Qi, L., Kennedy, A., 2006a. Subduction-related origin of the 750 Ma Xuelongbao adakitic complex (Sichuan Province, China): implications for the tectonic setting of the giant Neoproterozoic magmatic event in South China. Earth and Planetary Science Letters 248, 286–300.

Zhou, M.F., Ma, Y., Yan, D.P., Xia, X., Zhao, J.H., Sun, M., 2006b. The Yanbian Terrane (southern Sichuan Province, SW China): a Neoproterozoic arc assemblage in the western margin of the Yangtze Block. Precambrian Research 144, 19–38.

Zhou, M.F., Zhao, J.H., Xia, X.P., Sun, W.H., Yan, D.P., 2007. Comment on "Revisiting the "Yanbian Terrane": implications for Neoproterozoic tectonic evolution of the western Yangtze Block, South China" [Li et al. (2006)]. Precambrian Research 155, 153–157.